

Review

A Comprehensive Review on Efficiency Enhancement of Solar Collectors Using Hybrid Nanofluids

Abu Shadate Faisal Mahamude ¹, Muhamad Kamal Kamarulzaman ² , Wan Sharuzi Wan Harun ¹ ,
Kumaran Kadirgama ³, Devarajan Ramasamy ¹ , Kaniz Farhana ⁴ , Rosli Abu Bakar ⁴, Talal Yusaf ^{5,*} ,
Sivarao Subramanion ⁶ and Belal Yousif ⁷ 

- ¹ Department of Mechanical Engineering, College of Engineering, Universiti Malaysia Pahang, Gambang 26300, Pahang, Malaysia; mahamude.ump@gmail.com (A.S.F.M.); sharuzi@ump.edu.my (W.S.W.H.); deva@ump.edu.my (D.R.)
- ² Automotive Engineering Centre, Universiti Malaysia Pahang, Pekan 26600, Pahang, Malaysia; kamalkz@hotmail.com
- ³ Faculty of Mechanical and Automotive Engineering Technology, Universiti Malaysia Pahang, Pekan 26600, Pahang, Malaysia; kumaran@ump.edu.my
- ⁴ Department of Apparel Engineering, Bangladesh University of Textiles, Dhaka 1208, Bangladesh; kfarhana81@yahoo.com (K.F.); rosli@ump.edu.my (R.A.B.)
- ⁵ School of Engineering and Technology, Central Queensland University, Brisbane, QLD 4008, Australia
- ⁶ School of Engineering, Universiti Teknikal Malaysia Melaka, Durian Tunggal 76100, Melaka, Malaysia; sivarao@utem.edu.my
- ⁷ School of Engineering, The University Southern Queensland, Toowoomba, QLD 4350, Australia; belal.yousif@usq.edu.au
- * Correspondence: t.yusaf@cqu.edu.au



Citation: Mahamude, A.S.F.; Kamarulzaman, M.K.; Harun, W.S.W.; Kadirgama, K.; Ramasamy, D.; Farhana, K.; Bakar, R.A.; Yusaf, T.; Subramanion, S.; Yousif, B. A Comprehensive Review on Efficiency Enhancement of Solar Collectors Using Hybrid Nanofluids. *Energies* **2022**, *15*, 1391. <https://doi.org/10.3390/en15041391>

Academic Editor: Gianpiero Colangelo

Received: 31 December 2021

Accepted: 7 February 2022

Published: 14 February 2022

Publisher's Note: MDPI stays neutral with regard to jurisdictional claims in published maps and institutional affiliations.



Copyright: © 2022 by the authors. Licensee MDPI, Basel, Switzerland. This article is an open access article distributed under the terms and conditions of the Creative Commons Attribution (CC BY) license (<https://creativecommons.org/licenses/by/4.0/>).

Abstract: Because of its potential to directly transform solar energy into heat and energy, without harmful environmental effects such as greenhouse gas emissions. Hybrid nanofluid is an efficient way to improve the thermal efficiency of solar systems using a possible heat transfer fluid with superior thermo-physical properties. The object of this paper is the study the latest developments in hybrid applications in the fields of solar energy systems in different solar collectors. Hybrid nanofluids are potential fluids with better thermo-physical properties and heat transfer efficiency than conventional heat transfer fluids (oil, water, ethylene glycol) with single nanoparticle nanofluids. The research found that a single nanofluid can be replaced by a hybrid nanofluid because it enhances heat transfer. This work presented the recent developments in hybrid nanofluid preparation methods, stability factors, thermal improvement methods, current applications, and some mathematical regression analysis which is directly related to the efficiency enhancement of solar collector. This literature revealed that hybrid nanofluids have a great opportunity to enhance the efficiency of solar collector due to their noble thermophysical properties in replace of conventional heat transfer working fluids. Finally, some important problems are addressed, which must be solved for future study.

Keywords: hybrid nanofluids; efficiency; solar collectors; thermal properties

1. Introduction

A safe and prosperous world now needs more than ever an environmentally friendly and effective source of energy [1–3]. In the face of the challenges of eliminating fossil fuels and reducing exhaust emissions from those fuels, one of the major divisions of renewable energy is solar energy. Although the option of energy sources has always been low-priced, solar energy has never really been used globally. More to the point, while the energy of the sun is free, it is expected that the maintenance charge of such systems, including the construction of devices and systems, would surpass the total cost of the usable source [4–6]. Looking closely at renewable technologies and their recent development estimates, the world has a perceivable interest in solar energy systems, accounting for almost 60 percent of

the overall growth in the renewable energy potential of more than 250 GW in 2021–2022 [7]. There have been major efforts taken to increase the performance of the existing energy conversion systems [8,9].

In recent years, several academics and researchers have made progress in nano-fluid technologies. The number of papers published in the field of nano-fluids per year should be presented in Figure 1. The figure below illustrates the importance of nanofluid flows in the different engineering sectors as well as the solar energy sector. [10–20]. The evolution of technologies of nanofluids has drawn the attention of assorted researchers in recent years. With the aid of nanofluids, researchers have focused on research in many scientific fields, including warming, climate control, electronics and microelectronics, new energy, medicine, as well as energy and fuel management [21–26].

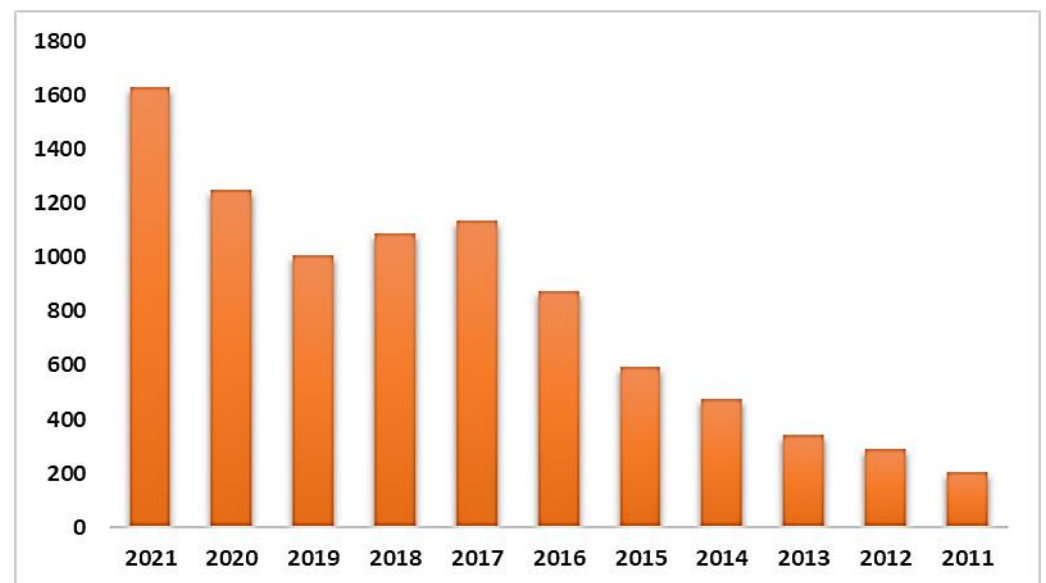


Figure 1. Schematic diagram of published articles in the Web of Science concerning with nanofluids.

The heat-transfer system plays a crucial role in many industries related to thermal and chemical processes. The heat-transfer process is always treated by using fluids. The main aim of the use of mixtures (hybrid nanofluid) is to improve the potency of the mixture's thermal properties, and the mixture of various nano-sized particles with fluid is called hybrid nanofluid. In practice, numerous methods have been applied to enhance the thermal properties of fluids. Nanoparticles are the most common and the most up-to-date technological trend in terms of improving heat-transfer efficiency [27]. Nanofluids have an excellent ability to increase the thermal efficiency of the solar collector by different nanoparticles used in different types of solar collectors [28]. Hybrid nanofluids were found to be the most efficient approach when used as a working fluid in solar energy systems [29]. The hybrid nanoparticles consist of a synthesis of two or more nanoparticles and are propagated into the base fluid. This is due to the synergistic effect of the hybrid nanofluid heat-transfer change compared to a nano-fluid containing a nano product. A hybrid nanofluid can have good thermal characteristics compared to the simple fluid and nanofluid-containing single nanoparticles [30]. The choice of the base fluid, size of nanoparticles, viscosity, fluid temperature and stability, dispensability of nanoparticles, purity of nanoparticles, method of preparation, size and shape of nanoparticles, and compatibility of nanoparticles have contributed significantly to the improvement of hybrid nanofluid heat transfer, resulting in the harmonious nanofluid mixture [31–35]. The primary goal of using hybrid nanofluids is to improve thermal conductivity at a lower cost and with acceptable stability due to the synergistic effect of its constituent materials. Stability is a term used to describe the long-term performance and thermal efficiency of nanofluids [36,37].

In comparison to mono nanofluids, hybrid nanofluids can significantly improve heat transmission. The pressure drop caused by the friction factor escalation, on the other hand, remains a major concern in hybrid nanofluids. The increase in pressure drop is a direct result of the increase in hybrid viscosity, which results in the penalty of high pumping power [30].

Nanoparticles are subject to various parameters of their thermal conductivity, including concentration, temperature, particle size, pH, shape, material, and perhaps, the production process. Theoretical models for thermal conductivity and viscosity determination. The stability of nanofluids or hybrid nanofluids in terms of settlement and agglomeration is still troublesome for practical applications, particularly in higher concentrations. Hybrid nanofluids, therefore, exhibit greater thermal conductivity compared to the individual nanofluids, which separately contain nanoparticles. Therefore, this paper focuses on evaluating the research of hybrid nano-fluid to recognize and resolve the latest technology by way of a forefront study into the economic feasibility of this technology in the future. The reported theoretical, digital, and experiential work on single nanofluid has revealed that nanofluid cooling, cameras, microcomputers, displays, heat exchangers, and space-craft applications can be implemented in various possible ways. Many thermal product reviews are found in the literature. However, single nanofluids are characterized and prepared. Few articles are available on hybrid nanofluid preparedness and thermal characteristics. The purpose of this paper is therefore to provide a further consideration of recent developments in various engineering applications in a hybrid nanofluid. Moreover, the critical challenges of hybrid nanofluids are presented, such as long-term stability, cost of preparation, and production. More experimental research is needed to address several issues related to hybrid nanofluids, such as instability and an increase in the friction factor, to reduce pumping power in solar systems. These issues appear to be critical for hybrid nanofluid commercialization and general applications. More importantly, the cost of preparing hybrid nanofluids is high and must be reduced. Future research should concentrate on finding a balance between the hybrid nanofluid's high thermal efficiency and the cost of preparation. This is a critical step toward the commercialization of hybrid nanofluids-based solar systems.

2. Historical Background

A key parameter of all the specifications which have contributed enormously to the improvement of heat transfer is thermal conductivity. Several studies have reported that the use of nanofluids has improved thermal conductivity undoubtedly [38–42]. Nanofluid hybrid is a brand-new type of nanofluid, which is massed by dispersing two distinct nanoparticles into an agreed heat-transference fluid. Hybrid nanofluids are possible fluids that have improved thermo-physical properties over traditional thermo-transfer fluids, an increased thermo-efficiency (oil, water, and ethylene glycol) and nanofluids with single nanoparticles. The scientific findings have shown that the hybrid nanofluid can be substituted with one single nanofluid as it enhances heat transfer, especially in the automotive, electro-mechanical, manufacturing, HVAC, and solar industries [43].

In solar collectors, a wide ranges of functioning fluids have been tested. Historically, water, grease, ethylene glycol, and various lubricants have been used to promote the performance of solar collectors, as shown in Figure 2 [44–49]. In anchor fluids (water, ethylene glycol or oil/lubricant), nanosized metals (Al, Cu, Zn, Ag, Au, etc.), metal oxides (SiO_2 , TiO_2 , Al_2O_3 , ZnO , CuO , etc.) or organic particles (carbon nanotubes, graphene oxide, diamond, etc. could be disseminated to create hybrid nanofluids) [50,51] are used to enhance the thermophysical properties and heat transfer efficiency, and hybrid nanofluid synthesis is crucial. The Al_2O_3 -Cu nanofluid, for example, was developed using the hydrogen reduction method using Al_2O_3 and CuO (90:10 ratio) to improve the viscosity to be steeper than concentration conductivity [52,53]. The MWCNT- Fe_3O_4 nanocomposite particle has been synthesized empirically (0–0.3 volume percentage) to test their thermal properties [54]. Improved thermal conductivity was achieved with Ag/MWCNT-HEG

hybrid nanofluids at 25 °C by 0.08 percent with 0.04 percent of volume fraction. The rheological properties of nanocomposite MWCNT-Ag can be measured by covalent and non-covalent working methods [55]. A 20.2% increase in the thermal transfer coefficient relative to the base fluid has been discovered in a platform exchanger by the MWCNT-TiO₂/water hybrid nanofluids [56]. The performance of the heat exchanger served by bringing together 0.0111% MWCNT/water nanofluid with 1.89% Al₂O₃/water. The appeal for graphene nanoplatelets (GNPs) has enormously increased despite the excellent use of MWCNTs for hybrid nanofluids [57]. Its diffusion in distilled water showed a 17.77% advancement in thermal conductivity at a 0.1% weight concentration and 40 °C. Another study investigated the impacts of particle concentration (range, 0.0–2.3%) and temperature (range, 25–50 °C) on the thermal conductivity of f-MWCNTs-Fe₃O₄-EG hybrid nanofluid [58]. The effects of various flows and geometrical parameters of solar thermal collector depend on different nanoparticles, base fluids and the thermophysical properties of different nanoparticles. This study indicated that the hybrid nanofluids significantly enhanced the exergy efficiency. The assessment criteria of the examined cases are the thermal, energetic, and overall performance and background of solar collector.

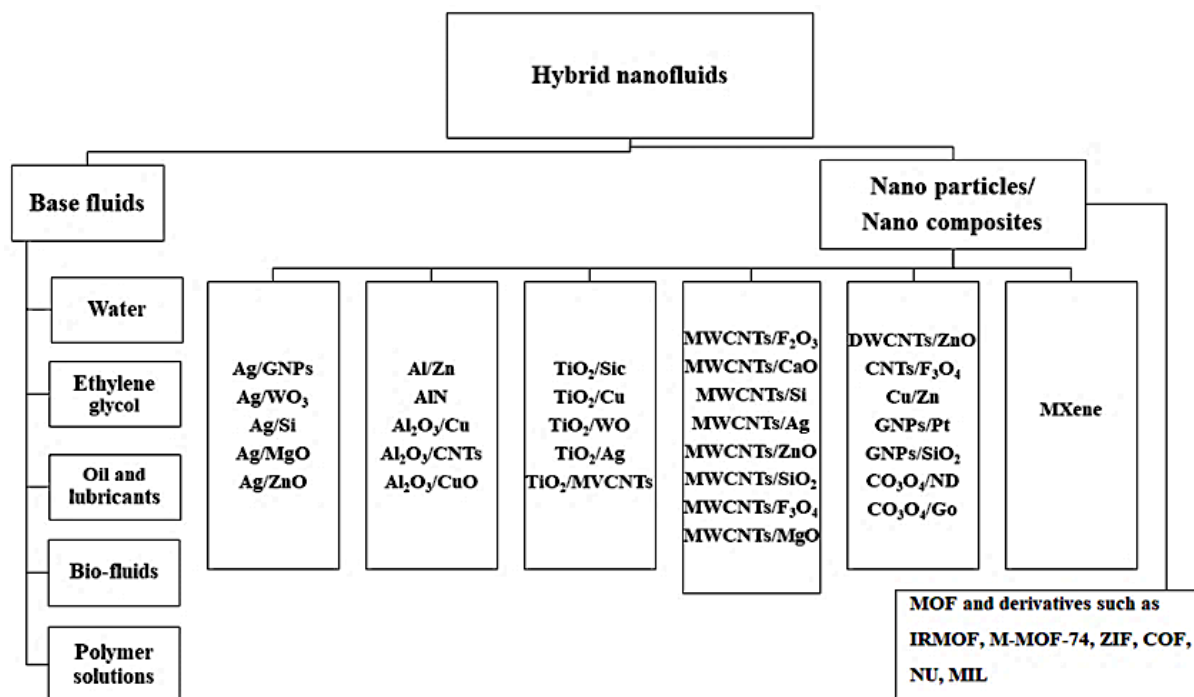


Figure 2. Scenario of different fluids and nanoparticles used for preparing hybrid nanofluids.

3. Preparation of Hybrid Nanofluids

Hybrid nanofluids are new fluids that are generated in a mixture or composite form to increase the heat transmission by suspending two or more nanoparticles [59]. By using hybrid nanostructures consisting of multiple materials with nano dimensions, the thermophysical properties of nanofluids can be further enhanced [43,60]. Water is the basic fluid exposed to radiation. This hybrid mixture uses a larger wavelength combination and absorbs heat. For various concentrations, diameters, and container heights, graphite and the numeric value for the mixture are added into the water of gold, silver, aluminum, graphite, and silicon dioxide gold nanoparticles [61]. Quite a few studies have studied and modeled the thermophysical characteristics of these hybrid fluid forms [62]. It has been found that relative to the base fluid at a volumetric concentration and a temperature of 0.86%, the thermal conductivity ratio of the hybrid nanofluid increased to 20.1% [63]. The reviewed literature indicates that hybrid nanofluids are an attractive candidate for thermal convective fluids in solar systems. Furthermore, hybrid nanofluids have a variety

of benefits, which make them more useful for the increase in heat transfer. A summary of solar power is given in this report. Subsequently, the use of hybrid nanofluids is reviewed and the findings are analyzed in various forms of solar-driven technologies [64]. The two-step process of nanofluid preparation includes the induction of the mechanical or chemical action of nanoparticles in powder form, followed mixing them with base fluid as shown in Figure 3. In the base fluid, powdered nanoparticles are dispersed by an intense shearing action known as ultrasonic. Both strength and ultrasonic length play a critical role in the stability of hybrid nanofluids [65].

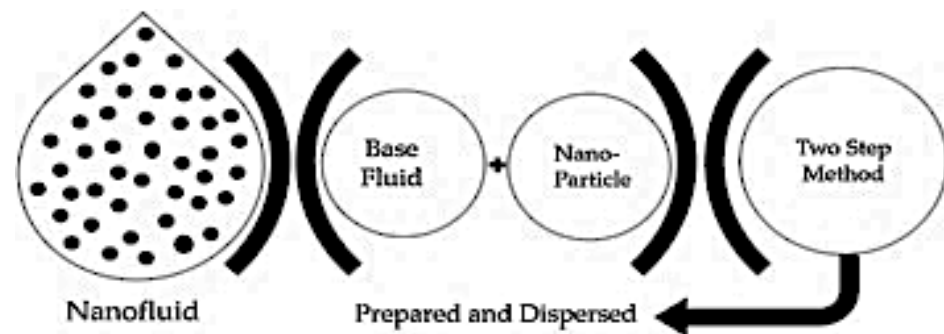


Figure 3. Portrayal of two-step method of nanofluid preparation [66].

By scattering around 0.2–1.5 vol.% of these nanoparticles in water and ethylene glycol, Al_2Cu , and Ag_2Al nanoparticles synthesized by mechanically alloying the prepared nanofluids, the nanoparticles were identified by X-ray diffraction and transmission electron microscopy and the nanofluid thermal conductivity was found by employing a changed thermal comparator. The findings suggest an increase in the thermal conductivity advancement of existing nanofluids by 50–150%. Both experimental findings and empirical analysis suggest that the degree of change strongly depends on the dispersed nanoparticles' identity/composition, scale, volume fraction, and shape [67]. The two-step method was used to generate a 0.1 percent volume fraction $\text{Al}_2\text{O}_3\text{-Cu}$ /water hybrid nanofluid. As a surfactant, sodium lauryl sulfate (SLS) was used. Before that, over several steps, a thermochemical synthesis process that included spray drying, precursor powder oxidation, hydrogen-atmosphere reduction, and homogenization was used to prepare the nanocrystalline alumina–copper ($\text{Al}_2\text{O}_3\text{-Cu}$) hybrid powder [68]. The two-step technique was introduced to generate identical hybrid nanofluids as prepared by Suresh et al. Dry f-MWCNT and nanoparticle Fe_3O_4 were prepared with a mixture of equivalent volumes. For the development of hybrid nanoparticles (f-MWCNT- Fe_3O_4) dispersed in ethylene glycol, a two-step method was employed [58].

MXene with a Ti_3C_2 chemical theorem was synthesized by applying the wet chemistry method and suspended in pure olein palm oil (OPO) to formulate a new type of heat-transfer fluid by applying COMSOL Metaphysics to investigate its thermal and energy efficiency numerically in a hybrid PV/T solar thermal structure. In addition to this research, the hybrid PV/T solar thermal device contrasts $\text{Al}_2\text{O}_3\text{-water}$ -based nanofluid with MXene-OPO nanofluid. With a loading concentration of 0.01, 0.03, 0.05, 0.08, 0.1, and 0.2 percent, the MXene-OPO nanofluid was prepared. At a 0.2 percent loading concentration, the MXene-OPO nanofluid exhibits a 68.5 percent higher thermal conductivity than pure OPO at 25 °C. When the temperature increased from 25 °C to 50 °C for the nanofluid with 0.2 wt. percent of MXene, the maximum viscosity reduction was observed as 61 percent. The MXene-based nanofluid shows about a 16 percent higher thermal efficiency improvement at a 0.07 kg/s flow rate compared to PVT with $\text{Al}_2\text{O}_3\text{-water}$ -based nanofluid. For the PVT with MXene nanofluids, a heat transfer coefficient improvement of approximately 9 percent was observed compared to PVT with $\text{Al}_2\text{O}_3\text{-water}$ heat-transfer fluid. Compared to the stand-alone PV modules, the MXene nanofluid can reduce PV temperature by 40 percent [69].

4. Application of Hybrid Nanofluids in the Solar Collector

The research related to the relevance of nanofluids is the talk of the hour. A research-facility survey of single nano-fluid work covering a wide range of functions has been carried out, with regard to electronic cooling, heat exchange, heat capacity, sun-based building heating and cooling, sun-powered pickers, cooling, room, and security, etc., [70–76]. Among all the applications, the usage, and the implementation of hybrid nanofluids in solar collectors are breaking new ground. The crossbreed or nanocomposite fluid may be a unique type of nanofluid, and although its utility at the research-facility level has been largely detailed in literary works [77–81], there is also work detailing factors such as heat exchange, electronic cooling, essential limits, and so on. It is now pertinent to focus on the mechanical utilization of crossbreed nano liquids with regard to single nano liquids [81] utilized such as Cu–TiO₂/deionized two-fold refined water hybrid nanofluid for ducts within the duct-sort counter stream heat exchanger. They detailed that the surface-functionalized and exceedingly crystalline nature of crossover nanocomposite (Cu–TiO₂) contributed to the creation of successful warm interfacing with the liquid medium; thus, allowing for the accomplishment of an increased heat conductivity and heat-transfer potential for nanofluids [79].

Concentrated solar panel (CSP) technology, as a typical PV application, is gaining popularity due to its benefits such as high conversion efficiency and low cost, among others. However, an important issue for CPV technology is non-uniformity in illumination and temperature, which can ultimately affect the overall electrical efficiency of solar cells [82]. Heat transfer applications have been analyzed by fluidic behavior, thermal properties, the size of nanoparticles and the mathematical co-relationships [83]. At higher temperatures, the increase in thermal conductivity with an increasing solid volume fraction is more pronounced. The effect of increasing the volume fraction on thermal conductivity, however, was greater than the effect of increasing temperature. Thermal conductivity was increased by 27.84% compared to the base fluid at a volume fraction of 0.5% and a temperature of 75 °C. Besides, Aguilar, Navas [84] studied the thermal properties of NiO-based nanofluids for CSP applications experimentally, and dynamic structures have also been studied as well. They inferred that thermal conductivity increased by up to 96% and that the heat transfer coefficient was enhanced by 50%. They also found that the surfactant has a significant effect on the improvement of thermal properties in CSP. Finally, a model for predicting the thermal conductivity of nanofluids based on the measured data was proposed. This model has a margin of error of 1.44 percent, indicating that the results obtained from model calculations are compatible with the experimental data [85]. The main criteria of the solar collector are to collect heat or increase the efficiency by using different nano or hybrid nanofluids of different conditions.

Table 1 illustrates the application characteristics of different solar collectors using hybrid nanofluids. For instance, FPC is used for warm-water in-home applications. Using hybrid nanofluids in these kinds of solar collectors enhances the productivity and outlet temperature, as well as the efficiency, which is also improved significantly. Additionally, ETSC is used to heat the water for residential purposes. ETSC is much better than FPC in cool weather. Generally, CPC is utilized for sun-oriented drying, water cleaning, and biomedical conditions, during which temperature performance is also increased by applying hybrid nanofluids. Besides, PTC is the most developed and commercially used solar collector. PTC is preferred largely due to some specific characteristics such as its high-temperature range. On the other hand, the linear frenal, parabolic-dish reflector, and heliostat-field collector are used to produce electricity by harvesting solar energy. These solar collectors perform at quite high temperatures.

Table 1. Application of hybrid nanofluids in various solar collectors.

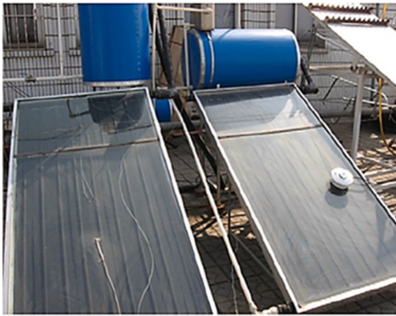
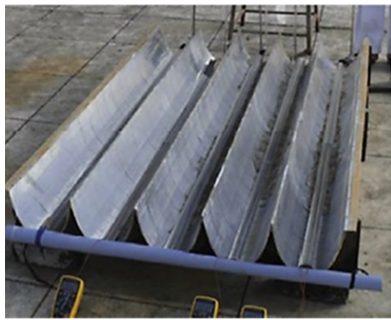


Reference	Types	Schematic Image	Applications
Tang, Cheng [86]	Flat-plate solar collector (FPSC)		Solar collector of this sort is abruptly utilized in residential hot water. Additionally, in manufacturing air deicer. 20–80 °C is the working temperature. Thus, it acts as foremost common sort of collector in different kinds of sun-oriented collector frameworks. Provides higher productivity and outlet temperatures when there is less warmth through the cover of glass in collector and the requirement of sunlight. Customary sorts are for the most part planned for warm climates. Efficiencies for 500 and 1000 W/m ² are 0.71–0.75 and 0.72–0.75 separately.
Arunkumar, Velraj [87]	Compound parabolic collector (CPC)		In terms of flow, these types are rather proficient in collection and concentration of far-off light sources, with a few acceptance points. Basic components in sun-oriented vitality collection, remote contact, sun-focused drying, water purification, biomedical, or any device involving condensation of a disparate source of light. It covers a temperature of 60–240 °C. 500 and 1000 W/m ² , with different efficiencies 0.45–0.73 and 0.58–0.72.
Papadimitratos, Sobhansarbandi [88]	Evacuated tube solar collector (ETSC)		These types are rather communal in residential hot water. Competent as air deicer. The working temperature of ETSC is 50–200 °C. They are more prudent than routine. In the cold weather, they provide more than FPC. Efficiencies of 500 W/m ² and 1000 W/m ² are between 0.44–0.82 and 0.62–0.82.
Li, Xu [89]	Parabolic trough collector (PTC)		Presently, as the most commercially used and most progressed, these types are rather proficient in control plants. Their capacity leads to the utilization of hybridization and vitality capacity by warm-vitality capacity. The preferences of PTC innovation incorporate the guarantee of the temperate venture, progressed innovation, ample operational involvement, and fossil-filling office and green energy sources. These have a temperature range of 400–500 °C.
Beltagy, Semmar [90]	Linear fresnel collector		These types play crucial roles in controlling plants. Currently, in the coordinated steam era, there is a predominance of utilizing this innovation compared to other sun-based frameworks, thereby reducing the cost of heat shift. The frame can be concentrated to provide surcharged steam. Significantly lower than the illustrative trough concentrators of 30–100, the defensive concentration variables are 10–40. Temperatures range between 100–450 °C.

Table 1. Cont.



Reference	Types	Schematic Image	Applications
Li, Dubowsky [91]	Parabolic dish reflector		This is simply defined as an electrical generator that generates daylight rather than coal or unrefined oil to create power. It was prepared with a dynamic following framework that can indicate the sun reliably. Temperatures can reach as high as 1500 °C.
Roca, de la Calle [92]	Heliostat field collector		Overheating during operation; costly choice for a broad range of operating applications including the development of solar energy, solar power, solar assist, carbon capture, water, and home applications. Temperature range of 12–85 °C.

Table 2 describes the research area and possible outcomes using hybrid nanofluids. Besides, Table 2 also presents the used nanoparticles and base fluids for these research studies. The repeatedly used nanoparticles are Al_2O_3 , MWCNT, Ag, Fe_3O_4 , MgO, SiO_2 , ZnO, TiO_2 , Cu, CNT, graphene, silica, and water is the most used base fluid. Ethylene glycol was also utilized several times as a base fluid in these research studies. Table 3 stated that research has been conducted in various areas such as in a circular tube, warm channel, electronic-warm sink, thermal solar collector, etc. Moreover, the thermo-physical properties such as optical and rheological properties of hybrid nanofluids are still being studied.

Table 2. Previous research works are based on hybrid nanofluids.

Author	Nanoparticles	Base Fluids	Research Study
Ho, Huang [80]	Al_2O_3 , MEPCM	Water	Crossbreed water, primarily based nanoparticle laminar in a round deportation
Han and Rhi [77]	Ag, Al_2O_3	Water	Considered warm characteristics for hybrid nanofluids on a notched warm channel.
Baby and Sundara [54]	Ag, HEG	HEG–Deionized water and Ethylene glycol (EG)	Improvement of heat physical phenomenon and warmth transfer for the arranged hybrid nanoparticle.
Esfe, Yan [93]	Ag, Al_2O_3	Water	Arrangement and characterization considered.
Selvakumar, Suresh [79], Suresh, Venkitaraj [94]	Cu, Al_2O_3	Water	Exploratory considerations of convective warm exchange and weight drop for crossbreed nanofluids in an electronic warm sink.

Table 2. Cont.

Author	Nanoparticles	Base Fluids	Research Study
Baghbanzadeh, Rashidi [95]	Silica, MWCNT	Distilled water	Heat transfer and weight drop for hybrid nanofluids in the associated electronic heat sink.
Chen, Yu [96]	Ag, MWCNT	Water	Considered the upgrade of compelling thermal conductivity.
Chen, Yu [96]	Graphene, MWCNT	Deionized water and Ethylene glycol (EG)	Upgrade of warm properties for hybrid nanofluids.
Jyothirmayee Aravind and Ramaprabhu [97]	Al ₂ O ₃ , MWCNT	water	Improvement of warm conductivity for single and half-breed nanofluids.
Munkhbayar, Tanshen [98]	Ag, MWCNT	Water	Examined the warm characteristics for the prepared cross breed nanofluids.
Labib, Nine [99]	CNT, Al ₂ O ₃	Water	Analytical examination along with the impact of associate fluids and cross-breed nanofluid in constrained convective heat exchange.
Tomar and Chakrabarty [100]	TiO ₂ , ZrO ₂	-	Considered the auxiliary and optical properties for the arranged nanocomposite.
Suresh, Venkitaraj [101]	Cu, Al ₂ O ₃	Distilled water	Turbulent warm exchange and weight sip for hybrid nanofluids in a consistently warmed round tube.
Madhesh, Parameshwaran [81]	Cu, TiO ₂	Water	Test considers convective heat transfer and natural philosophy characteristics of hybrid nanofluids in the tube heat exchanger.
Batmunkh, Tanshen [102]	MWCNT, Fe ₂ O ₃	Water	Tests consider heat-convective transfer and touch calculates nanofluids in a continuously warmed circular tube for a fully formed, turbulent stream on a crossover.
Xuan, Duan [103]	TiO ₂ , Ag	Water	Upgrade in sun-based assimilation.
Takabi and Salehi [73]	Cu, Al ₂ O ₃	Water	Considered the enlargement of the warm transfer performance of a sinusoidal corrugated enclosure by utilizing crossover nanofluid.
Baghbanzadeh, Rashidi [104]	Silica, MWCNT	Water	Considered the examination of an upgrade of rheological properties (thickness and density) for crossover nanofluids.
Sundar, Misganaw [105]	ND, NI	Water and EG	Examined the upgrade of thermal conductivity and thickness for the hybrid nanofluid with distinctive base liquids.
Syam Sundar, Sousa [106]	CNT, Fe ₃ O ₄	Water	Examined the warm exchange upgrade in low-quality awareness for the arranged hybrid nanofluids in a tube with bent tape inserts beneath turbulent steam.
Esfe, Wongwises [107]	Cu, TiO ₂	Water	Test examination of warm conductivity for the arranged crossover Nanofluids and created Artificial Neural Network (ANN) simulation and correlation for heat conductivity.
Esfe, Yan [93]	DWCNT, ZnO	Water	The heat conductivity improvement for the organized nanofluids examined for different temperatures (25 °C to 50 °C) and strong volume division of (0.25% to 1%).

Table 2. Cont.

Author	Nanoparticles	Base Fluids	Research Study
Esfe, Arani [108]	Ag, MgO	Water	Exploratory investigation on warm conductivity and energetic consistency for the arranged crossover Nanofluids with different volume divisions run from (0% to 2%) and created a relationship for warm conductivity and energetic thickness for the arranged cross breed nanofluids.
Afrand, Toghraie [109]	Fe ₃ O ₄ , Ag	EG	In particular, the effect on the rheological activity of the arranged blended nano-fluid is checked for temperature and nanoparticulate concentration.
Eshgarf, Afrand [110]	MWCNT, SiO ₂	EG-water	Experimental change of the temperature range (25 °C to 50 °C) from different suspensions to strong volume distribution and of the rheological behavior of non-Newtonian hybrid nano-coolants in heating and cooling frame applications from (0.0625% to 2%).
Harandi, Karimipour [58]	f-MWCNT, Fe ₃ O ₄	EG	The test considers the influence of temperature and concentration on the thermal conductivity of the arranged cross nanofluid from 25 °C to 50 °C, to test different tests of nanofluids with a volume fraction from 0.1% to 2.3% and unused produce. The relationship of the thermal conductivity of the fluid is considered for testing.
Sundar, Ramana [111]	ND, Fe ₃ O ₄	Water	Considered the improvement of warm conductivity, thickness for the arranged half-breed nanofluid by shifting the temperature ranges (20 °C to 60 °C) and the volume concentration (0.05 to 0.2%). Additionally, an unused relationship was established for the thermal conductivity and consistency of the semi-aligned nanofluid with exploratory information.
Soltani, Akbari [112]	MgO, MWCNT	EG	Exploratory consideration of energetic thickness for their arranged half-breed nanofluid with different volume concentrations (0.1% to 1%) by shifting the temperature (30 °C to 60 °C) and created an unused relationship for the energetic consistency from their experimental work.
Senniangiri, Bensam Raj [113,114]	Graphene/NiO	Coconut oil	The high nanomaterial concentration regenerates the formation of lamellar agglomerated particles and increases the complex viscosity of the basic fluid. To estimate the dynamism of the hybrid nanofluid with a limited deviation margin, it is suggested to use the theoretical correlation artificially (ANN).
Hussein, Habib [37]	Covalent functionalized graphene nanoplatelets	water	Found that when the mixed hybrid nanofluid was used as the absorption medium and the flow rate was 4 L/min, the solar collector with the highest thermal efficiency increased by as much as 85%.

Table 3. Previous research works are based on hybrid nanofluids.

Author	Base Fluid	Nanoparticles	Mass Volume %	Solar Collectors	Efficiency Observation
Harandi, Karimipour [58]	H ₂ O	Al ₂ O ₃ /Fe, Al ₂ O ₃	0.05–0.2 wt.	FPSC	Maximum 6.9% increase
Sundar, Misganaw [105]	H ₂ O	ND–CO ₃ O ₄	0.05–0.15 wt.	FPSC	Maximum 59% increase if 0.15 wt.
Hussein, Habib [37]	H ₂ O	MWCNTs/GNPs/h-BN	0.05–0.1 wt.	FPSC	Maximum 89% increase
[115]	H ₂ O	MWCNTs/MgO, MWCNTs/CuO	0.25–2 vol.	FPSC	Performance of CuO-MWCNT was 18.05%, while MgO-MWCNT was 20.52%.
Arkan, Abbasoğlu [116]	H ₂ O/EG	Al ₂ O ₃ , ZnO	0.25 vol.	FPSC	Performance was 15.13% positive
[117]	H ₂ O	SWCNT	0.2 vol.	ETSC	Optimum productivity at 93.43%
[118]	H ₂ O	Al ₂ O ₃ , TiO ₂	0.3 wt.	ETSC	Compared to its based liquid, the system's performance improved by 16.67%
Daghigh and Zandi [119]	H ₂ O	MWCNT, CuO and TiO ₂	Different	ETSC	Performance of the collector using nanoparticles MWCNT, CuO, and TiO ₂ , compared to water, increased by 25%, 12%, and 5%, respectively.
Peng, Zahedidastjerdi [120]	Water	Al ₂ O ₃ , CuO, TiO ₂	Different	ETSC	CuO has 1.5% higher collector thermal efficiency than Al ₂ O ₃ , TiO ₂ -water fluid
Luo, Wang [121]	Oil	C, Ag, SiO ₂ , Al ₂ O ₃ , Cu	0.01–0.025 wt.	DAC	Efficiency improves by 30–100 K and by 2–25% than the base oil
Hussain, Jawad [122]	H ₂ O	Ag and ZrO ₂	5 vol.	ETSC	Efficiency % not mentioned but improved.
Kim, Ham [123]	20% propylene glycol-water	MWCNT, Al ₂ O ₃ , CuO, SiO ₂ , and TiO ₂	0.2 vol.	ETSC	Performance 20% increase
Kaya, Gürel [124,125]	Methanol	CuO	0.3 vol.	Tube	Performance 63% increase
Gorji and Ranjbar [126,127]	water	Graphite, Magnetite—15 nm, Silver—20 nm	5–40 ppm	DAC	According to the results, nanofluids promoted thermal and exergy efficiencies by 33–57% and 13–20%, respectively, compared to base fluid.
Li, Chang [128]	Di-water	Ti ₃ AlC ₂ , hydrochloric acid, triton X—100	100 ppm	DAC	For MXene loading, the maximum photothermal conversion efficiency of 77.49% is achieved.

Table 3. Cont.

Author	Base Fluid	Nanoparticles	Mass Volume %	Solar Collectors	Efficiency Observation
Samylingam, Aslfattahi [69]	Di-water	Ti ₃ AlC ₂ , plum oil—MXene-OPO	0.2 wt.	DAC	A 40% efficiency increase with respect to Al ₂ O ₃ -water-based nanofluid.
Gupta, Singh [129]	Water	ZnFe ₂ O ₄	0.02–0.5 wt.	DAC	Performance enhancement of 42.99%
Abdelrazik, Tan [130]	Di-water	rGO-Ag, graphene oxide	0.0005 to 0.05 wt.	DAC	Hybrid system displays improved efficiency at concentrations of less than 0.0235 wt. percent compared to the PV system without integration with optical filtration. The hybrid solar PV/T system with OF using water/rGO-Ag nanofluid can produce thermal energy with efficiencies between 24 percent and 30 percent.
Kasaeian, Daneshazarian [131]	EG	Nano silica	0.3 wt.	PTC	Maximum outlet temperature of MWCNT is 338.3 K, and the thermal performance reaches 74.9%.
Loni, Pavlovic [132]	Water	TiO ₂ , SiO ₂ , Fe ₂ O ₃ , ZnO, Al ₂ O ₃ .	N/A	PTC	Use pure water to enhance the energy performance of low enthalpy parabolic trough collectors.
Esfe, Alirezaie [133]	EG	SWCNT-MgO	0.05–2 vol.	PTC	Thermal conductivity enhancement of 18%.
Bahrami, Akbari [24]	EG-water	Fe-CuO	0.05–1.5 wt.	PTC	Efficiency increases in the different conditions in different types.
[134]	Engine oil	MWCNT-ZnO	0.125–1.0 wt.	PTC	If the viscosity increases then the efficiency increases.
Afrand [135]	EG	MgO-MWCNT	0.6 vol.	PTC	Performance increase—21%
Sundar, Singh [136]	EG-water	graphene oxide/CO ₃ O ₄	0.2 vol.	PTC	Performance increase—water based—19.14% Performance increase—EG based 11.75%
Nine, Batmunkh [137]	Water	Al ₂ O ₃ -MWCNT	1–6 wt.	PTC	Increasing thermal conductivity is not sharp when compared to simple nanofluids
Baby and Sundara [54]	Water and EG	CuO-HEG	0.05 vol.	PTC	Increasing thermal conductivity with volume fraction
Khan, Abid [138]	Oil-based	Al ₂ O ₃ , CuO and TiO ₂	1 wt.	Solar dish collector	Performance increased by 33.73% and 36.27%
Loni, Pavlovic [132]	Thermal oil	Cu, CuO, TiO ₂ , and Al ₂ O ₃	0–5 wt.	Solar dish collector	Thermal efficiency is found to be equivalent to 35% and up to 10% of the exergy efficiency.

Table 3. Cont.

Author	Base Fluid	Nanoparticles	Mass Volume %	Solar Collectors	Efficiency Observation
Zadeh, Sokhansefat [139]	Synthesis oil/thermal oil	Al ₂ O ₃	N/A	Tube	Improve the mean efficiency by 4.25%.
Huang and Marefati [140]	Thermal oil and water	CuO and Al ₂ O ₃	N/A	Solar dish collector	Efficiency increase—28.7%
Loni, Asli-Ardeh [141]	Thermal oil	Al ₂ O ₃ /thermal, SiO ₂ /thermal	N/A	Solar dish collector	Improve efficiency
Potenza, Milanese [142]	Airflow	CuO, nanopowder	N/A	Transparent receiver tube	Mean efficiency of about 65%
Aslfattahi, Samyilingam [143]	Silicon oil	MXene with a chemical formula of Ti ₃ C ₂	0.1 wt.	Photovoltaic thermal collector	Thermal conductivity improvement of 64%.
Soltani, Kasaieian [144]	Water	SiO ₂ , Fe ₃ O ₄	N/A	Photovoltaic thermal-thermoelectric system	Maximum energy efficiency at the fixed irradiation of 900 W/m ² .
Sardarabadi, Passandideh-Fard [145]	Water	SiO ₂	1–3 wt.	Photovoltaic thermal-thermoelectric system	Total exergy of the PV/T system with nanofluids was increased by up to 24.31%.
Arora, Singh [146]	Water	SWCNT, MWCNT NP	Different	Photovoltaic thermal-thermoelectric system	Percentage enhancement in total yield obtained using SWCNT and MWCNT was 65.7% and 28.1%, respectively.
Wahab, Khan [147]	Water	Graphene hybrid	0.05–0.15 vol.	Hybrid photovoltaic thermal system.	Maximum sustainability index of 1.17 is shown at optimum conditions.
Soltani, Kasaieian [148]	Water	SiO ₂ , Fe ₃ O ₄	Mass ratio 0.5 vol.	Photovoltaic thermal collector	Improvement of 54.29% and 1.72% in both power production and efficiency.
Sardarabadi, Hosseinzadeh [149]	Water	Al ₂ O ₃ , TiO ₂ , ZnO	0.2 wt.	Photovoltaic thermal collector	Results indicate that the overall exergy efficiencies for the cases of PVT/water, PVT/TiO ₂ , PVT/Al ₂ O ₃ , and PVT/ZnO are enhanced by 12.34%, 15.93%, 18.27%, and 15.45%, respectively
Sardarabadi, Passandideh-Fard [150]	Water	TiO ₂ , ZnO, Al ₂ O ₃	0.2	Photovoltaic thermal collector	Performance of ZnO is better than for the other types. The numerical model shows that the mass fraction of hybrid nanofluid has a significant impact on the thermal performance of PVT collectors.

5. Efficiency Observations of Solar Collectors with Hybrid Nanofluids

Hybrid nanofluid and thermal systems play a vital role in heat transfer and the efficiency enhancement of solar collector. Efficiency enhancement is also directly related to nanoparticle size and the mass flow system of fluid, concentration or solid volume fraction of nanoparticles may have a significant effect on the thermal conductivity of hybrid

nanofluids. [116]. When a hybrid nanofluid was prepared using $\text{Al}_2\text{O}_3/\text{Fe}$, Al_2O_3 -water, with the mass volume of 0.05–0.2 wt., the volume % increases the efficiency of thermal heat transfer by 6.9%, as found by Harandi, Karimipour [58]. The hybrid nanofluids were developed by dispersing a synthetic ND- CO_3O_4 nanocomposite into water, ethylene glycol, and water mixtures to confirm the ND and CO_3O_4 phases of synthesized nanocomposites. The thermal properties including thermal conductivity and viscosity were experimentally tested at various weight and temperature concentrations and the ND- CO_3O_4 -water maximum efficiency increased to 59% if 0.15 wt. as found by Sundar, Misganaw [105]. The efficiency increased to 89% for the water-based MWCNTs/GNPs/h-BN flat plate solar collector, whereas the mass volume concentration was 0.05 to 0.1 for the weight of water, as reported by Hussein, Habib [37]. For the water-based MWCNTs/MgO, MWCNTs/CuO flat-plate solar collector, the mass volume concentration was 0.25 to 0.2% wt., and the performance increase of CuO-MWCNT was 18.05%, while for MgO-MWCNT it was 20.52% [117]. An efficiency increase of 15.13% was observed for the water/EG-based Al_2O_3 , ZnO flat-plate solar collector, whereas the mass volume concentration was 0.25, as reported by Arıkan, Abbasođlu [116]. Recent studies have investigated this kind of solar collector. The use of hybrid nanofluids is studied in the planned method, and some of the problems in some of the ETSCs with increased heat transfer are evaluated through the general analysis, such as different types of nano-fluids, the nano-fluid scale, volume-fraction, and hybrid nano-fluid application. The efficiency of ETSCs was affected by nanoparticles, using a base fluid [117–124]. In some studies, the enhanced performance was attributed to a higher Nusselt number. The Nusselt number can be improved with the use of hybrid nanofluids to make convective heat transfer more efficient [125,126].

6. Mathematical Analysis of Hybrid Nanofluids in Solar Collectors

When sunbeams, G , hit the darkened absorber's surface zone, A_{ab} , they are ingested by the heat-exchange medium and transferred into the heat. The valuable vitality selected by the collector, Q_u , is the sum of warmth that the working liquid collects, subtracted by the sum of the heat exchange from the collector to the discussion as the misplaced vitality [151–153].

$$\eta_{FPC} = \frac{Q_c}{AcG} = \frac{mCp(T_o - T_i)}{AcG} \quad (1)$$

where F_R is calculated as

$$F_R = \frac{mCp}{A_{ab}} \left(1 - \exp \left[\frac{U_L F' Ac}{mCp} \right] \right) \quad (2)$$

and T_{ab} and T_a are the surface temperature of the safeguard and discuss temperature individually, F' indicates the collector proficiency figure which drops with a rise in the general misfortune coefficient, U_L , from the accepting plate to the environment, which was firstly presented by Hottel and Woertz [154] that was afterward created by Klein [155].

$$U_L = U_{to} + U_{bo} + U_{ed} \quad (3)$$

Hence, the valuable vitality extricated from the collector can be decided by the sum of the sun-oriented occurrence where the warm productivity of an FPC can be assessed as provided by Fudholi, Sopian [156].

$$\eta_{FPC} = \frac{Q_c}{AcG} = \frac{mCp(T_o - T_i)}{AcG} \quad (4)$$

where η (%) is the collector effectiveness, Q_c is the vitality achieved from the collector, m is the mass stream rate, C_p is the heat, Ac is the collector range, T_o and T_i are the outlet and gulf temperatures of the liquid separately. In TSCs, the safeguard range is an imperative parameter characterized as the plate region short the punctured range and demonstrates the sum of the retained vitality ($Q_{ab} = GA\alpha\epsilon$). Radiative and convective heat traded from

the surface to the encompassing and the back divider are the major components for warm misfortunes [157,158]. For this sort, heat productivity is portrayed as a division of the overall sun-powered energy that comes to the collector's surface and is accomplished by the discussion as the valuable heat which can be calculated as demonstrated by Leon and Kumar [159].

$$\eta_{FPC} = \frac{m_a C_{p,a} (T_{a,o} - T_{amb})}{(T_{abs} - T_{amb})} \quad (5)$$

A further calculation of the warm trade adequacy (HEE) proportion (ϵ_{HX}) is additionally taken under consideration to assess the contrast between the real temperature and the greatest conceivable esteem given by Kutscher [160].

$$\epsilon_{HX} = \frac{(T_{a,o} - T_{amb})}{(T_{abs} - T_{amb})} \quad (6)$$

Solar collectors are one of the cleanest and most efficient heating systems available. Density, absorbency, temperature, the heat-transmission system, dynamic viscosity and types of nanoparticles are important for efficiency. Table 4 just illustrates the different parameter, which are directly related to efficiency. Normally, temperature and volume are the key parameters of the solar collector co-relation. Besides, if we see an example analysis of hybrid nanofluids as shown in Figure 4, we can see that depending on nanoparticle concentration, it depicts the thermal conductivity of hybrid nanofluids. Remarkable researchers preserved tiny quantities of nanoparticles to prevent particle sedimentation and agglomeration (usually less than 1%). At 1.5% of the volume, the maximal increase in thermal conductivity for Al₂Cu hybrid nanofluids was 150 percent. Nanoparticle weight and volume % is the key to the hybrid nanofluid performance of enhancing heat efficiency. can The mathematical correlations related to the design of the solar collector, numerical simulations, efficiency enhancement of solar collectors with different variables such as volume concentrations and viscosity are presented in Table 4.

Table 4. Mathematical expression of solar collectors.

References	Specification	Correlation	Remarks
Esfe, Behbahani [161]	Functioning fluid: SiO ₂ -MWCNT/EG Temperature field: 30–50 °C Volume area: 0.05–1.95 vol. %	$\frac{A_{nf}}{K_{bf}}$ $= 0.905 + 0.002069\varphi T$ $+ 0.04375\varphi^{0.09265} T^{0.3305}$ $- 0.0063\varphi^3$	Two design methods and a feed-forward neural network have been provided to model the thermal conductivity of the hybrid nanofluid. R ² values of 0.9864 and 0.9981 were obtained for new methods and the artificial neural network (ANN). When these two measurement methods were compared to experimental data, both methods proved to be effective in predicting data. However, ANN's correlation findings have a much lower error.
Afrand [135]	Functioning fluid: MgO-MWCNT/EG Temperature field: 25–50 °C Volume area: 0–0.6 vol. %	$\frac{A_{nf}}{K_{bf}} = 0.8341 + 1.1\varphi^{0.243} T^{-0.289}$	Maximum increase in nanofluid thermal conductivity is 21.3%. A new connection was proposed to estimate the nanofluid thermal conductivity.
Sardarabadi, Passandideh-Fard [150]	Functioning fluid: f-MWCNTs-Fe ₃ O ₄ /EG Temperature field: 25–50 °C Volume range: 0–2.3 vol. %	$\frac{A_{nf}}{K_{bf}} = 1 + 0.0162\varphi^{0.7038} T^{0.6009}$	Numerical simulation has been validated and used for the effects of mass ZnO-nanoparticles on TiO ₂ , ZnO, Al ₂ O ₃ /water nanofluids (0.2 wt.%).

Table 4. Cont.

References	Specification	Correlation	Remarks
Esfahani, Toghraie [162]	Functioning fluid: ZnO-Ag/H ₂ O Temperature range: 25–50 °C Volume range: 0.125–2 vol. %	$\frac{A_{nf}}{K_{bf}} = 1 + 0.00008794\phi^{0.5899} T^{1.345}$	Effect on thermal conductivity of hybrid nanofluid of volume fractions and temperatures is demonstrated.
Toghraie, Chaharsoghi [163]	Functioning fluid: ZnO-Ag/H ₂ O Temperature field: 25–50 °C Volume percentage: 0–3.5 vol. %	$\frac{A_{nf}}{K_{bf}} = 1 + 0.004503\phi^{0.8717} T^{0.7972}$	Increase in thermal conductivity variance of nano-fluids with a higher solid volume fraction temperature is also greater than that of a lower solid volume fraction.
Alirezaie, Saedodin [164]	Functioning fluid: f-MWCNT-MgO/engine oil Volume percentage: 0.0625–1 vol. % Heat range: 25–50 °C Shear rate: 50–650 rpm	$\mu_{nf} = 4 \times 10^4 + 145\phi - 240T - 0.061\gamma + 1.9 \times 10^6 \phi^2 + 0.36 T^2$	Experimental data were calculated with a three-variable correlation, with artificial neural networks modeling the experimental results. The comparison of experimental results with the simulations shows that neural-network modeling is highly accurate.
Asadi, Asadi [134]	Functioning fluid: f-MWCNT-ZnO/engine oil Volume percentage: 0.125–1 vol. % Heat variable: 5–55 °C	$\mu_{nf} = 796.8 + 76.26\phi + 12.88T + 0.7695\phi T + \frac{-196.9T - 16.53\phi T}{T^{0.8441}}$	At a solid concentration of 2 percent and a temperature of 40 °C, a maximal increase in dynamic viscosity was achieved at 65% while a minimum increase in solid concentration was achieved at 0.25% and a temperature of 25 °C was achieved at 14.4%.
Esfe, Arani [62]	Functioning fluid: MWCNT-ZnO/10W40 engine oil Volume percentage: 0.05–1 vol. % Temperature difference: 5–55 °C	$\frac{\mu_{nf}}{\mu_{bf}} = 1.035 + \frac{\phi e^{-1.023} \left(\frac{2.046\phi}{T} + 0.4015\phi^2 T \right)}{T^{0.8441}}$	Thermal conductivity at some temperatures was 38% higher than that of ethylene glycol. A new correlation of volume concentration and temperature ($R^2 = 0.9925$) is proposed to forecast experimental thermal conductivity.
Moldoveanu, Ibanescu [165]	Functioning fluid: Al ₂ O ₃ -SiO ₂ /H ₂ O	For 0.5% Al ₂ O ₃ + 0.5% SiO ₂ : $\mu_{nf} = 0.000005T^2 - 0.003T + 0.5$ For 0.5% Al ₂ O ₃ + 1.5% SiO ₂ : $\mu_{nf} = 0.00000T^2 - 0.004T + 0.571$	Temperature variation in viscosity for hybrid nanofluid, which underpins viscosity reduction as the temperature increase rises and the action of low hysteresis, has been studied experimentally, proposing two viscosity variation equations as the temperature increases.
Motahari, Moghaddam [166,167]	Functioning fluid: MWCNT-SiO ₂ /20W50 oil Volume range: 0.05–1 vol. % Heat range: 40–100 °C	$\frac{\mu_{nf}}{\mu_{bf}} = 0.09422 - \left[\left(\frac{T}{\phi} \right)^2 + 0.100556 T^{0.8827} \phi^{0.3148} \right] \exp(72474.75T\phi^{3.7951})$	Increase in solid volume fraction and temperature-improved hybrid nano-lubricant viscosity. Nano viscosity was 171 percent higher than pure 20W50, at its maximum solid volume fraction and temperature. Current models are not capable of predicting the hybrid viscosity of nano-lubricants. A new correlation was thus suggested with an R-squared of 0.9943 with regard to solid volume fraction and temperature.

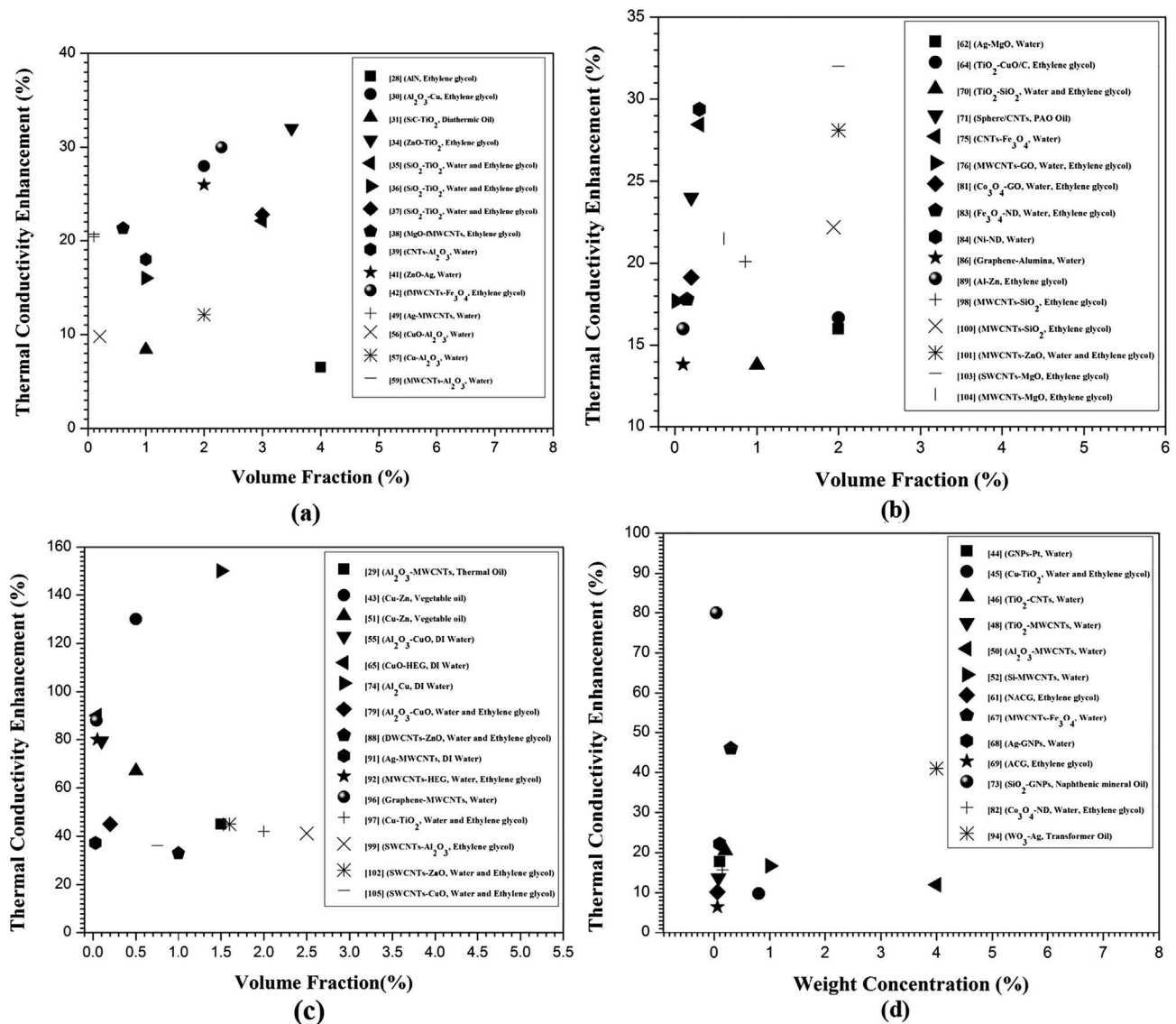


Figure 4. Enhancement of thermal conductivity using hybrid nanofluids; (a–c) mirror an accelerated thermal conductivity as a feature of the quantity fraction of the thermal conductivity improvement obtained via researchers (d) as a characteristic of the obtained weight fraction [167].

7. Challenges Found Based on the Study

Hybrid nanofluids are newly emerging dynamic liquids, which remain in the study stage. Researchers continue, however, to conduct a feasibility analysis on hybrid nanofluids and solar collectors for better performance across different applications. Some interesting characteristics of hybrid nanofluids were noticed in the performance of heat transfer but there are some challenges with regard to them being a new type of working fluid. First, there is a lack of consensus between researchers and the theoretical model to predict the exact behavior of hybrid nanofluids. Second, there is a lack of understanding between the researchers. Third, in the preparation process, the findings for a particular hybrid nanofluid and volume fraction vary in different methods. The challenges include the design of the solar plate, mixing and making the concentration of the base fluid with different nanoparticles, whether it flows inside the tube or coil, the stability of the hybrid nanofluid, the behavior of surfactants usage, nanoparticles size and volume concentration, pumping power, pressure drop, and most importantly, the cost of hybrid nanofluids.

7.1. Physical Characteristics

Stability is one of the main factors in the success of nanofluids and can have a detrimental impact on the hybrid nanofluid, i.e., lack of good stability. The stability of certain nanofluids deteriorates over time, which was observed by previous researchers. Surfactants were used to minimize fluid surface tension and to promote the dispersibility of particles in a fluid [53] or no active surface compound. Excess surfactant, however, affects nanofluid viscosity, thermal conductive properties, and stability [168]. Solar power systems are also based on the mass and size of nanoparticles [169]. More research on the effect of nanoparticles on solar energy has been reported for thermal systems [170]. Reference has been made to the appropriate size and quantity of nanoparticles required to optimize the maximum outlet temperature and achieve the desired thermal efficiency of the solar collector [146].

Nanofluids can be prepared by calculating the number of nanoparticles for the required volume concentrations using the following (Equation (7)) [171]:

$$\phi = \left[\frac{\frac{w}{\rho_p}}{\frac{w}{\rho_p} + \frac{w_{bf}}{\rho_{bf}}} \right] \times 100 \quad (7)$$

where ϕ is the volume concentration of nanofluids (%); w is the mass; and ρ stands for the density of nanoparticles. The subscripts p and bf stand for nanoparticles and base fluid, respectively.

A visual inspection of sedimentation in the GNP nanofluids was performed, and it was indicated that the GNP nanofluids were stable even after the heat-transfer run [172] examined the stability of the nanofluids by observing the sedimentation photographs of the nanofluids captured after 30 days of preparation [173]. A combined experimental and statistical method was used to investigate the effective thermal conductivity and relative viscosity of CNC/W-EG nanofluids. The authors used a sedimentation observation to assess the stability of nanofluids. The observation was carried out every day in this investigation. After one week of preparation of the nanofluids, there was no aggregation of CNC and Al_2O_3 nanoparticles at the bottom of the test tube, as portrayed in Figure 5. This discovery reveals the moderate to good stability of both nanofluids, whereas quantitative approaches have been used to study the numerical values of stability as shown in Figure 6 [42].

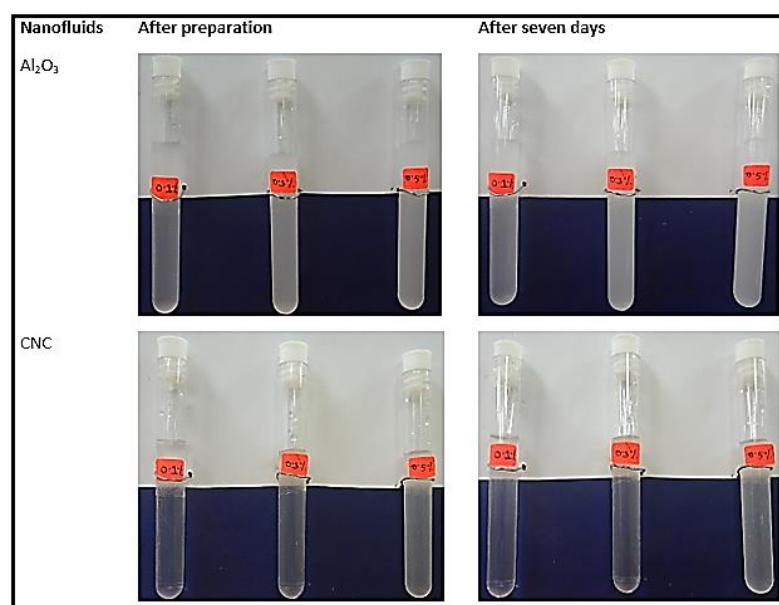


Figure 5. Evaluation of qualitative stability measurement of nanofluids [42].

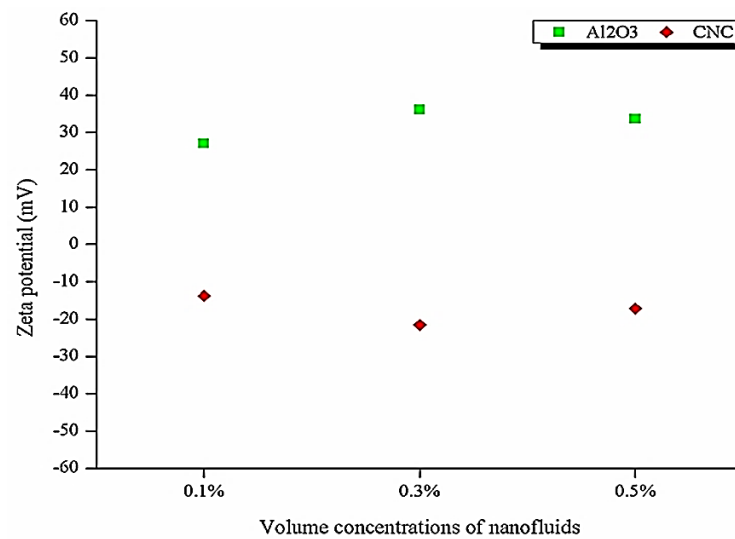


Figure 6. Quantitative analysis of the stability of nanofluids [42].

7.2. Design and Mathematical Relationship

The total efficiency of the solar collector is based on the design parameters. The evaluation of the efficiency of each upgrading technique centered on the characteristics concerned. Thus, with characteristics such as a higher concentration rate, the effect of sun trackers may be more positive [174]. Hybrid nanoparticles have volume functions in most of the correlations formed by experiments. The efficiency in the heat transfer was characterized by hybrid nanofluids. However, there exist some disagreements with regard to the development of hybrid nanofluids as a new working fluid replacing water or any common working fluid. Besides, the results of a similar hybrid nanofluid analysis appeared to have little contrast as regards to thermal improvement. In particular, the data gained by different researchers are not standardized. Furthermore, expected mathematical correlations are still limited for other applications because of their limitations. The experimental application of nanofluids is therefore limited. Mathematical models rely solely on experimental integrity analytical research [175].

7.3. Cost and Economic Perspective

An economic analysis is used to identify industrial effective nanofluids. It is especially critical, therefore, that the type and price of hybrid nanofluids are considered so that the best comprehensive thermal transfer efficiency can be achieved at a lower cost for further industrial applications [176]. The mixing of nanoparticles and preparation of hybrid nanofluids is a challenge in the cost-effective procedure [177]. More importantly, the cost of creating hybrid nanofluids is prohibitively expensive and must be reduced. Future research should focus on finding a balance between the high thermal efficiency of the hybrid nanofluid and the cost of preparation.

8. Conclusions

In this current paper, a comprehensive study has been performed on the performance of solar collectors with hybrid nanofluids. The literature reviewed that hybrid nanofluids had been applied in different engineering fields to enhance their performance in terms of the circular tube, heat channel, electronic-heat sink and thermal solar collector. Moreover, hybrid nanofluids were implemented in various kinds of solar collectors such as a flat-plate collector, compound parabolic collector, evacuated tube solar collector, parabolic trough collector, linear Fresnel collector, parabolic-dish reflector, and heliostat field collector to evaluate the performance in replace of conventional fluids. The study mainly stated the performance of efficiency of solar collectors that has been increased significantly. A maximum increase of 89% efficiency was achieved for a flat-plate collector by MWCNTs/GNPs/h-

BN-water hybrid nanofluids. The stable, higher thermal conductive, and lower viscous hybrids nanofluids are preferred so as to improve the performance of a solar collector. Although the hybrid can increase the efficiency of solar collectors to a greater extent, it is also associated with some obstacles. However, a hybrid nanofluid is an impressive fluid to replace conventional fluids and increase the efficiency of solar collectors.

Author Contributions: Conceptualization, A.S.F.M. and W.S.W.H.; resources, M.K.K.; data curation, K.K.; writing—original draft preparation, D.R. and A.S.F.M.; writing—review and editing, K.F.; visualization, R.A.B.; supervision, W.S.W.H.; project administration, T.Y.; funding acquisition, S.S. and B.Y. All authors have read and agreed to the published version of the manuscript.

Funding: This research was funded by [Ministry of Higher Education of Malaysia] grant number [FRGS/1/2019/TK03/UMP/02/15] and Universiti Malaysia Pahang internal grant [RDU213308]. The APC was funded by [RDU1903134]. Information regarding the funder and the funding number should be provided. Please check the accuracy of funding data and any other information carefully.

Institutional Review Board Statement: Not applicable.

Informed Consent Statement: Not applicable.

Data Availability Statement: Not applicable.

Conflicts of Interest: The authors declare no conflict of interest.

References

- Furlan, C.; Mortarino, C. Forecasting the impact of renewable energies in competition with non-renewable sources. *Renew. Sustain. Energy Rev.* **2018**, *81*, 1879–1886. [[CrossRef](#)]
- Elsaid, K.; Sayed, E.T.; Abdelkareem, M.A.; Baroutaji, A.; Olabi, A. Environmental impact of desalination processes: Mitigation and control strategies. *Sci. Total Environ.* **2020**, *740*, 140125. [[CrossRef](#)] [[PubMed](#)]
- Elsaid, K.; Sayed, E.T.; Abdelkareem, M.A.; Mahmoud, M.S.; Ramadan, M.; Olabi, A. Environmental impact of emerging desalination technologies: A preliminary evaluation. *J. Environ. Chem. Eng.* **2020**, *8*, 104099. [[CrossRef](#)]
- Olfian, H.; Ajarostaghi, S.S.M.; Ebrahimnataj, M. Development on evacuated tube solar collectors: A review of the last decade results of using nanofluids. *Sol. Energy* **2020**, *211*, 265–282. [[CrossRef](#)]
- Plante, R.H. *Solar Energy, Photovoltaics, and Domestic Hot Water: A Technical and Economic Guide for Project Planners, Builders, and Property Owners*; Academic Press: Cambridge, MA, USA, 2014.
- Wilberforce, T.; Baroutaji, A.; El Hassan, Z.; Thompson, J.; Soudan, B.; Olabi, A. Prospects and challenges of concentrated solar photovoltaics and enhanced geothermal energy technologies. *Sci. Total Environ.* **2018**, *659*, 851–861. [[CrossRef](#)]
- International Energy Agency. *Renewable Energy Market Update*; International Energy Agency: Paris, France, 2022.
- Olabi, A.; Elsaid, K.; Rabaia, M.K.H.; Askalany, A.A.; Abdelkareem, M.A. Waste heat-driven desalination systems: Perspective. *Energy* **2020**, *209*, 118373. [[CrossRef](#)]
- Brough, D.; Mezquita, A.; Ferrer, S.; Segarra, C.; Chauhan, A.; Almahmoud, S.; Khordehghah, N.; Ahmad, L.; Middleton, D.; Sewell, H.I.; et al. An experimental study and computational validation of waste heat recovery from a lab scale ceramic kiln using a vertical multi-pass heat pipe heat exchanger. *Energy* **2020**, *208*, 118325. [[CrossRef](#)]
- Bandyopadhyay, S.; Chakraborty, S. Thermophoretically driven capillary transport of nanofluid in a microchannel. *Adv. Powder Technol.* **2018**, *29*, 964–971. [[CrossRef](#)]
- Esmaeili, E.; Rounaghi, S.A.; Gruner, W.; Eckert, J. The preparation of surfactant-free highly dispersed ethylene glycol-based aluminum nitride-carbon nanofluids for heat transfer application. *Adv. Powder Technol.* **2019**, *30*, 2032–2041. [[CrossRef](#)]
- Al-Rashed, A.A.; Ranjbarzadeh, R.; Aghakhani, S.; Soltanimehr, M.; Afrand, M.; Nguyen, T.K. Entropy generation of boehmite alumina nanofluid flow through a minichannel heat exchanger considering nanoparticle shape effect. *Phys. A Stat. Mech. Its Appl.* **2019**, *521*, 724–736. [[CrossRef](#)]
- Purusothaman, A. Investigation of natural convection heat transfer performance of the QFN-PCB electronic module by using nanofluid for power electronics cooling applications. *Adv. Powder Technol.* **2018**, *29*, 996–1004. [[CrossRef](#)]
- Mahdi, J.M.; Lohrasbi, S.; Ganji, D.D.; Nsofor, E.C. Simultaneous energy storage and recovery in the triplex-tube heat exchanger with PCM, copper fins and Al₂O₃ nanoparticles. *Energy Convers. Manag.* **2018**, *180*, 949–961. [[CrossRef](#)]
- Mei, S.; Qi, C.; Luo, T.; Zhai, X.; Yan, Y. Effects of magnetic field on thermo-hydraulic performance of Fe₃O₄-water nanofluids in a corrugated tube. *Int. J. Heat Mass Transf.* **2018**, *128*, 24–45. [[CrossRef](#)]
- Wang, G.; Qi, C.; Liu, M.; Li, C.; Yan, Y.; Liang, L. Effect of corrugation pitch on thermo-hydraulic performance of nanofluids in corrugated tubes of heat exchanger system based on exergy efficiency. *Energy Convers. Manag.* **2019**, *186*, 51–65. [[CrossRef](#)]
- Qi, C.; Liu, M.; Tang, J. Influence of triangle tube structure with twisted tape on the thermo-hydraulic performance of nanofluids in heat-exchange system based on thermal and exergy efficiency. *Energy Convers. Manag.* **2019**, *192*, 243–268. [[CrossRef](#)]

18. Farhana, K.; Kadirgama, K.; Rahman, M.M.; Noor, M.M.; Ramasamy, D.; Samykano, M.; Najafi, G.; Sidik, N.A.C.; Tarlochan, F. Significance of alumina in nanofluid technology. *J. Therm. Anal.* **2019**, *138*, 1107–1126. [[CrossRef](#)]
19. Abu-Hamdeh, N.H.; Alazwari, M.A.; Salilih, E.M.; Sajadi, S.M.; Karimipour, A. Improve the efficiency and heat transfer rate' trend prediction of a flat-plate solar collector via a solar energy installation by examine the Titanium Dioxide/Silicon Dioxide-water nanofluid. *Sustain. Energy Technol. Assess.* **2021**, *48*, 101623. [[CrossRef](#)]
20. Ashour, A.F.; El-Awady, A.T.; Tawfik, M.A. Numerical investigation on the thermal performance of a flat plate solar collector using ZnO & CuO water nanofluids under Egyptian weathering conditions. *Energy* **2021**, *240*, 122743. [[CrossRef](#)]
21. Khodadadi, H.; Aghakhani, S.; Majd, H.; Kalbasi, R.; Wongwises, S.; Afrand, M. A comprehensive review on rheological behavior of mono and hybrid nanofluids: Effective parameters and predictive correlations. *Int. J. Heat Mass Transf.* **2018**, *127*, 997–1012. [[CrossRef](#)]
22. Arani, A.A.A.; Akbari, O.A.; Safaei, M.R.; Marzban, A.; Alrashed, A.A.; Ahmadi, G.R.; Nguyen, T.K. Heat transfer improvement of water/single-wall carbon nanotubes (SWCNT) nanofluid in a novel design of a truncated double-layered microchannel heat sink. *Int. J. Heat Mass Transf.* **2017**, *113*, 780–795. [[CrossRef](#)]
23. Khodabandeh, E.; Safaei, M.R.; Akbari, S.; Akbari, O.A.; Alrashed, A.A. Application of nanofluid to improve the thermal performance of horizontal spiral coil utilized in solar ponds: Geometric study. *Renew. Energy* **2018**, *122*, 1–16. [[CrossRef](#)]
24. Bahrami, M.; Akbari, M.; Karimipour, A.; Afrand, M. An experimental study on rheological behavior of hybrid nanofluids made of iron and copper oxide in a binary mixture of water and ethylene glycol: Non-Newtonian behavior. *Exp. Therm. Fluid Sci.* **2016**, *79*, 231–237. [[CrossRef](#)]
25. Ranjbarzadeh, R.; Karimipour, A.; Afrand, M.; Isfahani, A.H.M.; Shirneshan, A. Empirical analysis of heat transfer and friction factor of water/graphene oxide nanofluid flow in turbulent regime through an isothermal pipe. *Appl. Therm. Eng.* **2017**, *126*, 538–547. [[CrossRef](#)]
26. Dehkordi, R.A.; Esfe, M.H.; Afrand, M. Effects of functionalized single walled carbon nanotubes on thermal performance of antifreeze: An experimental study on thermal conductivity. *Appl. Therm. Eng.* **2017**, *120*, 358–366. [[CrossRef](#)]
27. Nazir, U.; Nawaz, M.; Alharbi, S.O. Thermal performance of magnetohydrodynamic complex fluid using nano and hybrid nanoparticles. *Phys. A Stat. Mech. Its Appl.* **2020**, *553*, 124345. [[CrossRef](#)]
28. Farhana, K.; Kadirgama, K.; Rahman, M.M.; Ramasamy, D.; Noor, M.M.; Najafi, G.; Samykano, M.; Mahamude, A.S.F. Improvement in the performance of solar collectors with nanofluids—A state-of-the-art review. *Nano-Struct. Nano-Objects* **2019**, *18*, 100276. [[CrossRef](#)]
29. Shah, T.R.; Ali, H.M. Applications of hybrid nanofluids in solar energy, practical limitations and challenges: A critical review. *Sol. Energy* **2019**, *183*, 173–203. [[CrossRef](#)]
30. Sarkar, J.; Ghosh, P.; Adil, A. A review on hybrid nanofluids: Recent research, development and applications. *Renew. Sustain. Energy Rev.* **2015**, *43*, 164–177. [[CrossRef](#)]
31. Zainal, S.; Tan, C.; Sian, C.; Siang, T.J. ANSYS simulation for Ag/HEG hybrid nanofluid in turbulent circular pipe. *J. Adv. Res. Appl. Mech.* **2016**, *23*, 20–35.
32. Li, H.; Ha, C.-S.; Kim, I.J. Fabrication of carbon nanotube/SiO₂ and carbon nanotube/SiO₂/Ag nanoparticles hybrids by using plasma treatment. *Nanoscale Res. Lett.* **2009**, *4*, 1384–1388. [[CrossRef](#)]
33. Karthikeyan, N.; Philip, J.; Raj, B. Effect of clustering on the thermal conductivity of nanofluids. *Mater. Chem. Phys.* **2008**, *109*, 50–55. [[CrossRef](#)]
34. Sastry, N.N.V.; Bhunia, A.; Sundararajan, T.; Das, S.K. Predicting the effective thermal conductivity of carbon nanotube based nanofluids. *Nanotechnology* **2008**, *19*, 055704. [[CrossRef](#)] [[PubMed](#)]
35. Sidik, N.A.C.; Adamu, I.M.; Jamil, M.M. Preparation methods and thermal performance of hybrid nanofluids. *J. Adv. Res. Appl. Mech.* **2020**, *66*, 7–16. [[CrossRef](#)]
36. Chakraborty, S.; Panigrahi, P.K. Stability of nanofluid: A review. *Appl. Therm. Eng.* **2020**, *174*, 115259. [[CrossRef](#)]
37. Hussein, O.A.; Habib, K.; Muhsan, A.S.; Saidur, R.; Alawi, O.A.; Ibrahim, T.K. Thermal performance enhancement of a flat plate solar collector using hybrid nanofluid. *Sol. Energy* **2020**, *204*, 208–222. [[CrossRef](#)]
38. Choi, S.U.S.; Zhang, Z.G.; Yu, W.; Lockwood, F.E.; Grulke, E.A. Anomalous thermal conductivity enhancement in nanotube suspensions. *Appl. Phys. Lett.* **2001**, *79*, 2252–2254. [[CrossRef](#)]
39. Azwadi, C.N.; Adamu, I.J. Turbulent force convective heat transfer of hybrid nano fluid in a circular channel with constant heat flux. *J. Adv. Res. Fluid Mech. Therm. Sci.* **2016**, *19*, 1–9.
40. Lee, Y.J. The use of nanofluids in domestic water heat exchanger. *J. Adv. Res. Appl. Mech.* **2014**, *3*, 9–24.
41. Park, S.D.; Lee, S.W.; Kang, S.; Bang, I.C.; Kim, J.H.; Shin, H.S.; Lee, D.W. Effects of nanofluids containing graphene/graphene-oxide nanosheets on critical heat flux. *Appl. Phys. Lett.* **2010**, *97*, 023103. [[CrossRef](#)]
42. Farhana, K.; Kadirgama, K.; Mohammed, H.A.; Ramasamy, D.; Samykano, M.; Saidur, R. Analysis of efficiency enhancement of flat plate solar collector using crystal nano-cellulose (CNC) nanofluids. *Sustain. Energy Technol. Assess.* **2021**, *45*, 101049. [[CrossRef](#)]
43. Sidik, N.A.C.; Jamil, M.M.; Japar, W.M.A.A.; Adamu, I.M. A review on preparation methods, stability and applications of hybrid nanofluids. *Renew. Sustain. Energy Rev.* **2017**, *80*, 1112–1122. [[CrossRef](#)]
44. Budihardjo, I.; Morrison, G.L.; Behnia, M. Natural circulation flow through water-in-glass evacuated tube solar collectors. *Sol. Energy* **2007**, *81*, 1460–1472. [[CrossRef](#)]

45. Minardi, J.E.; Chuang, H.N. Performance of a “black” liquid flat-plate solar collector. *Sol. Energy* **1975**, *17*, 179–183. [[CrossRef](#)]
46. Singh, A.K.J. A review study of solar desalting units with evacuated tube collectors. *J. Clean. Prod.* **2020**, *279*, 123542. [[CrossRef](#)]
47. Zhou, Y.; Li, Q.; Wang, Q. Energy storage analysis of UIO-66 and water mixed nanofluids: An experimental and theoretical study. *Energies* **2019**, *12*, 2521. [[CrossRef](#)]
48. McGrail, B.; Thallapally, P.K.; Blanchard, J.; Nune, S.; Jenks, J.; Dang, L. Metal-organic heat carrier nanofluids. *Nano Energy* **2013**, *2*, 845–855. [[CrossRef](#)]
49. García, E.J.; Bahamon, D.; Vega, L.F. Systematic search of suitable metal–organic frameworks for thermal energy-storage applications with low global warming potential refrigerants. *ACS Sustain. Chem. Eng.* **2021**, *9*, 3157–3171. [[CrossRef](#)]
50. Murshed, S.S.J. Correction and comment on “thermal conductance of nanofluids: Is the controversy over?”. *J. Nanopart. Res.* **2009**, *11*, 511–512. [[CrossRef](#)]
51. Amrollahi, A.; Rashidi, A.; Meibodi, M.E.; Kashefi, K. Conduction heat transfer characteristics and dispersion behaviour of carbon nanofluids as a function of different parameters. *J. Exp. Nanosci.* **2009**, *4*, 347–363. [[CrossRef](#)]
52. Suresh, S.; Venkitaraj, K.P.; Selvakumar, P.; Chandrasekar, M. Synthesis of Al₂O₃–Cu/water hybrid nanofluids using two step method and its thermo physical properties. *Colloid. Surf. A Physicochem. Eng. Asp.* **2011**, *388*, 41–48. [[CrossRef](#)]
53. Sundar, L.S.; Singh, M.K.; Sousa, A.C.J. Enhanced heat transfer and friction factor of MWCNT–Fe₃O₄/water hybrid nanofluids. *Int. Commun. Heat Mass Transf.* **2014**, *52*, 73–83. [[CrossRef](#)]
54. Baby, T.T.; Sundara, R.J. Synthesis and transport properties of metal oxide decorated graphene dispersed nanofluids. *J. Phys. Chem. C* **2011**, *115*, 8527–8533. [[CrossRef](#)]
55. Amiri, A.; Shanbedi, M.; Eshghi, H.; Heris, S.Z.; Baniadam, M. Highly dispersed multiwalled carbon nanotubes decorated with Ag nanoparticles in water and experimental investigation of the thermophysical properties. *J. Phys. Chem. C* **2012**, *116*, 3369–3375. [[CrossRef](#)]
56. Huang, D.; Wu, Z.; Sunden, B. Effects of hybrid nanofluid mixture in plate heat exchangers. *Exp. Therm. Fluid Sci.* **2016**, *72*, 190–196. [[CrossRef](#)]
57. Yarmand, H.; Gharekhani, S.; Ahmadi, G.; Shirazi, S.F.S.; Baradaran, S.; Montazer, E.; Zubir, M.N.M.; Alehashem, M.; Kazi, S.; Dahari, M. Graphene nanoplatelets–silver hybrid nanofluids for enhanced heat transfer. *Energy Convers. Manag.* **2015**, *100*, 419–428. [[CrossRef](#)]
58. Harandi, S.S.; Karimipour, A.; Afrand, M.; Akbari, M.; D’Orazio, A.J. An experimental study on thermal conductivity of F-MWCNTs–Fe₃O₄/EG hybrid nanofluid: Effects of temperature and concentration. *Int. Commun. Heat Mass Transf.* **2016**, *76*, 171–177. [[CrossRef](#)]
59. Ahammed, N.; Asirvatham, L.G.; Wongwises, S.J. Entropy generation analysis of graphene–alumina hybrid nanofluid in multiport minichannel heat exchanger coupled with thermoelectric cooler. *Int. J. Heat Mass Transf.* **2016**, *103*, 1084–1097. [[CrossRef](#)]
60. Maddah, H.; Aghayari, R.; Mirzaee, M.; Ahmadi, M.H.; Sadeghzadeh, M.; Chamkha, A.J. Factorial experimental design for the thermal performance of a double pipe heat exchanger using Al₂O₃–TiO₂ hybrid nanofluid. *Int. Commun. Heat Mass Transf.* **2018**, *97*, 92–102. [[CrossRef](#)]
61. Tullius, T.K.; Bayazitoglu, Y. Analysis of a hybrid nanofluid exposed to radiation. *Numer. Heat Transf. Part B Fundam.* **2016**, *69*, 271–286. [[CrossRef](#)]
62. Esfe, M.H.; Arani, A.A.A.; Badi, R.S.; Rejvani, M.J. ANN modeling, cost performance and sensitivity analyzing of thermal conductivity of DWCNT–SiO₂/EG hybrid nanofluid for higher heat transfer. *J. Therm. Anal. Calorim.* **2018**, *131*, 2381–2393. [[CrossRef](#)]
63. Esfe, M.H.; Rejvani, M.; Karimpour, R.; Arani, A.A.A. Estimation of thermal conductivity of ethylene glycol-based nanofluid with hybrid suspensions of SWCNT–Al₂O₃ nanoparticles by correlation and ANN methods using experimental data. *J. Therm. Anal.* **2017**, *128*, 1359–1371. [[CrossRef](#)]
64. Ahmadi, M.H.; Ghazvini, M.; Sadeghzadeh, M.; Alhuyi Nazari, M.; Ghalandari, M. Utilization of hybrid nanofluids in solar energy applications: A review. *Nano-Struct. Nano-Objects* **2019**, *20*, 100386. [[CrossRef](#)]
65. Sidik, N.A.C.; Adamu, I.M.; Jamil, M.M.; Kefayati, G.H.; Mamat, R.; Najafi, G. Recent progress on hybrid nanofluids in heat transfer applications: A comprehensive review. *Int. Commun. Heat Mass Transf.* **2016**, *78*, 68–79. [[CrossRef](#)]
66. Ali, H.M.; Babar, H.; Shah, T.R.; Sajid, M.U.; Qasim, M.A.; Javed, S. Preparation techniques of TiO₂ nanofluids and challenges: A review. *Appl. Sci.* **2018**, *8*, 587. [[CrossRef](#)]
67. Chopkar, M.; Kumar, S.; Bhandari, D.; Das, P.; Manna, I. Development and characterization of Al₂Cu and Ag₂Al nanoparticle dispersed water and ethylene glycol based nanofluid. *Mater. Sci. Eng. B* **2007**, *139*, 141–148. [[CrossRef](#)]
68. Moghadassi, A.; Ghomi, E.; Parvizian, F. A numerical study of water based Al₂O₃ and Al₂O₃–Cu hybrid nanofluid effect on forced convective heat transfer. *Int. J. Therm. Sci.* **2015**, *92*, 50–57. [[CrossRef](#)]
69. Samyalingam, L.; Aslfattahi, N.; Saidur, R.; Yahya, S.M.; Afzal, A.; Arifutzzaman, A.; Tan, K.; Kadirgama, K. Thermal and energy performance improvement of hybrid PV/T system by using olein palm oil with MXene as a new class of heat transfer fluid. *Sol. Energy Mater. Sol. Cells* **2020**, *218*, 110754. [[CrossRef](#)]
70. Brailsford, A.D.; Major, K.G. The thermal conductivity of aggregates of several phases, including porous materials. *Br. J. Appl. Phys.* **1964**, *15*, 313–319. [[CrossRef](#)]
71. Miles, J., Jr.; Robertson, H.J. The dielectric behavior of colloidal particles with an electric double-layer. *Phys. Rev.* **1932**, *40*, 583. [[CrossRef](#)]

72. Takabi, B.; Salehi, S.J. Augmentation of the heat transfer performance of a sinusoidal corrugated enclosure by employing hybrid nanofluid. *Adv. Mech. Eng.* **2014**, *6*, 147059. [[CrossRef](#)]
73. Yu, W.; Xie, H. A review on nanofluids: Preparation, stability mechanisms, and applications. *J. Nanomater.* **2012**, *2012*, 1–17. [[CrossRef](#)]
74. Wong, K.V.; De Leon, O.J. Applications of nanofluids: Current and future. *Adv. Mech. Eng.* **2010**, *2*, 519659. [[CrossRef](#)]
75. Wen, D.; Lin, G.; Vafaei, S.; Zhang, K. Review of nanofluids for heat transfer applications. *Particuology* **2009**, *7*, 141–150. [[CrossRef](#)]
76. Saidur, R.; Leong, K.Y.; Mohammed, H.A. A review on applications and challenges of nanofluids. *Renew. Sustain. Energy Rev.* **2011**, *15*, 1646–1668. [[CrossRef](#)]
77. Han, W.; Rhi, S. Thermal characteristics of grooved heat pipe with hybrid nanofluids. *Therm. Sci.* **2011**, *15*, 195–206. [[CrossRef](#)]
78. He, Y.; Vasiraju, S.; Que, L. Hybrid nanomaterial-based nanofluids for micropower generation. *RSC Adv.* **2013**, *4*, 2433–2439. [[CrossRef](#)]
79. Selvakumar, P.; Suresh, S. Use of Al₂O₃-Cu/water hybrid nanofluid in an electronic heat sink. *IEEE Trans. Compon. Packag. Manuf. Technol.* **2012**, *2*, 1600–1607. [[CrossRef](#)]
80. Ho, C.; Huang, J.; Tsai, P.; Yang, Y. On laminar convective cooling performance of hybrid water-based suspensions of Al₂O₃ nanoparticles and MEPCM particles in a circular tube. *Int. J. Heat Mass Transf.* **2011**, *54*, 2397–2407. [[CrossRef](#)]
81. Madhesh, D.; Parameshwaran, R.; Kalaiselvam, S. Experimental investigation on convective heat transfer and rheological characteristics of Cu-TiO₂ hybrid nanofluids. *Exp. Therm. Fluid Sci.* **2014**, *52*, 104–115. [[CrossRef](#)]
82. Li, G.; Xuan, Q.; Pei, G.; Su, Y.; Ji, J. Effect of non-uniform illumination and temperature distribution on concentrating solar cell—A review. *Energy* **2017**, *144*, 1119–1136. [[CrossRef](#)]
83. Said, Z.; Ghodbane, M.; Sundar, L.S.; Tiwari, A.K.; Sheikholeslami, M.; Boumeddane, B.J. Heat transfer, entropy generation, economic and environmental analyses of linear Fresnel reflector using novel rGO-Co₃O₄ hybrid nanofluids. *Renew. Energy* **2021**, *165*, 420–437. [[CrossRef](#)]
84. Aguilar, T.; Navas, J.; Sánchez-Coronilla, A.; Martín, E.I.; Gallardo, J.J.; Martínez-Merino, P.; Gómez-Villarejo, R.; Piñero, J.C.; Alcántara, R.; Fernández-Lorenzo, C.J. Investigation of enhanced thermal properties in NiO-based nanofluids for concentrating solar power applications: A molecular dynamics and experimental analysis. *Appl. Energy* **2018**, *211*, 677–688. [[CrossRef](#)]
85. Bakhtiari, R.; Kamkari, B.; Afrand, M.; Abdollahi, A. Preparation of stable TiO₂-graphene/water hybrid nanofluids and development of a new correlation for thermal conductivity. *Powder Technol.* **2021**, *385*, 466–477. [[CrossRef](#)]
86. Tang, R.; Cheng, Y.; Wu, M.; Li, Z.; Yu, Y. Experimental and modeling studies on thermosiphon domestic solar water heaters with flat-plate collectors at clear nights. *Energy Convers. Manag.* **2010**, *51*, 2548–2556. [[CrossRef](#)]
87. Arunkumar, T.; Velraj, R.; Denkenberger, D.; Sathyamurthy, R.; Kumar, K.V.; Ahsan, A. Productivity enhancements of compound parabolic concentrator tubular solar stills. *Renew. Energy* **2016**, *88*, 391–400. [[CrossRef](#)]
88. Papadimitratos, A.; Sobhansarbandi, S.; Pozdin, V.; Zakhidov, A.; Hassanipour, F. Evacuated tube solar collectors integrated with phase change materials. *Sol. Energy* **2016**, *129*, 10–19. [[CrossRef](#)]
89. Li, X.; Xu, E.; Ma, L.; Song, S.; Xu, L. Modeling and dynamic simulation of a steam generation system for a parabolic trough solar power plant. *Renew. Energy* **2019**, *132*, 998–1017. [[CrossRef](#)]
90. Beltagy, H.; Semmar, D.; Lehaut, C.; Said, N. Theoretical and experimental performance analysis of a Fresnel type solar concentrator. *Renew. Energy* **2017**, *101*, 782–793. [[CrossRef](#)]
91. Li, L.; Dubowsky, S. A new design approach for solar concentrating parabolic dish based on optimized flexible petals. *Mech. Mach. Theory* **2011**, *46*, 1536–1548. [[CrossRef](#)]
92. Roca, L.; de la Calle, A.; Yebra, L.J.J. Heliostat-field gain-scheduling control applied to a two-step solar hydrogen production plant. *Appl. Energy* **2013**, *103*, 298–305. [[CrossRef](#)]
93. Esfe, M.H.; Yan, W.-M.; Akbari, M.; Karimipour, A.; Hassani, M.J. Experimental study on thermal conductivity of DWCNT-ZnO/water-EG nanofluids. *Int. Commun. Heat Mass Transf.* **2015**, *68*, 248–251. [[CrossRef](#)]
94. Suresh, S.; Venkataraj, K.P.; Selvakumar, P.; Chandrasekar, M. Effect of Al₂O₃-Cu/water hybrid nanofluid in heat transfer. *Exp. Therm. Fluid Sci.* **2012**, *38*, 54–60. [[CrossRef](#)]
95. Baghbanzadeh, M.; Rashidi, A.; Rashtchian, D.; Lotfi, R.; Amrollahi, A. Synthesis of spherical silica/multiwall carbon nanotubes hybrid nanostructures and investigation of thermal conductivity of related nanofluids. *Thermochim. Acta* **2012**, *549*, 87–94. [[CrossRef](#)]
96. Chen, L.; Yu, W.; Xie, H. Enhanced thermal conductivity of nanofluids containing Ag/MWNT composites. *Powder Technol.* **2012**, *231*, 18–20. [[CrossRef](#)]
97. Aravind, S.S.J.; Ramaprabhu, S. Graphene wrapped multiwalled carbon nanotubes dispersed nanofluids for heat transfer applications. *J. Appl. Phys.* **2012**, *112*, 124304. [[CrossRef](#)]
98. Munkhbayar, B.; Tanshen, R.; Jeoun, J.; Chung, H.; Jeong, H. Surfactant-free dispersion of silver nanoparticles into MWCNT-aqueous nanofluids prepared by one-step technique and their thermal characteristics. *Ceram. Int.* **2013**, *39*, 6415–6425. [[CrossRef](#)]
99. Labib, M.N.; Nine, J.; Afrianto, H.; Chung, H.; Jeong, H. Numerical investigation on effect of base fluids and hybrid nanofluid in forced convective heat transfer. *Int. J. Therm. Sci.* **2013**, *71*, 163–171. [[CrossRef](#)]
100. Tomar, L.J.; Chakrabarty, B. Synthesis, structural and optical properties of TiO₂-ZrO₂ nanocomposite by hydrothermal method. *Adv. Mater. Lett.* **2013**, *4*, 64–67. [[CrossRef](#)]

101. Suresh, S.; Venkitaraj, K.P.; Hameed, M.S.; Sarangan, J. Turbulent heat transfer and pressure drop characteristics of dilute water based Al_2O_3 -Cu hybrid nanofluids. *J. Nanosci. Nanotechnol.* **2014**, *14*, 2563–2572. [[CrossRef](#)]
102. Batmunkh, M.; Tanshen, R.; Nine, J.; Myekhlai, M.; Choi, H.; Chung, H.; Jeong, H. Thermal conductivity of TiO_2 nanoparticles based aqueous nanofluids with an addition of a modified silver particle. *Ind. Eng. Chem. Res.* **2014**, *53*, 8445–8451. [[CrossRef](#)]
103. Xuan, Y.; Duan, H.; Li, Q.J. Enhancement of solar energy absorption using a plasmonic nanofluid based on TiO_2/Ag composite nanoparticles. *RSC Adv.* **2014**, *4*, 16206–16213. [[CrossRef](#)]
104. Baghbanzadeh, M.; Rashidi, A.; Soleimanisalim, A.H.; Rashtchian, D. Investigating the rheological properties of nanofluids of water/hybrid nanostructure of spherical silica/MWCNT. *Thermochim. Acta* **2014**, *578*, 53–58. [[CrossRef](#)]
105. Sundar, L.S.; Misganaw, A.H.; Singh, M.K.; Sousa, A.C.M.; Ali, H.M. Efficiency analysis of thermosyphon solar flat plate collector with low mass concentrations of ND- Co_3O_4 hybrid nanofluids: An experimental study. *J. Therm. Anal.* **2020**, *143*, 959–972. [[CrossRef](#)]
106. Syam Sundar, L.; Sousa, A.; Singh, M.K. Heat transfer enhancement of low volume concentration of carbon nanotube- Fe_3O_4 /water hybrid nanofluids in a tube with twisted tape inserts under turbulent flow. *J. Therm. Sci. Eng. Appl.* **2015**, *7*, 021015. [[CrossRef](#)]
107. Esfe, M.H.; Wongwises, S.; Naderi, A.; Asadi, A.; Safaei, M.R.; Rostamian, H.; Dahari, M.; Karimipour, A. Thermal conductivity of Cu/ TiO_2 -water/EG hybrid nanofluid: Experimental data and modeling using artificial neural network and correlation. *Int. Commun. Heat Mass Transf.* **2015**, *66*, 100–104. [[CrossRef](#)]
108. Esfe, M.H.; Arani, A.A.A.; Rezaie, M.; Yan, W.-M.; Karimipour, A. Experimental determination of thermal conductivity and dynamic viscosity of Ag-MgO/water hybrid nanofluid. *Int. Commun. Heat Mass Transf.* **2015**, *66*, 189–195. [[CrossRef](#)]
109. Afrand, M.; Toghraie, D.; Ruhani, B. Effects of temperature and nanoparticles concentration on rheological behavior of Fe_3O_4 -Ag/EG hybrid nanofluid: An experimental study. *Exp. Therm. Fluid Sci.* **2016**, *77*, 38–44. [[CrossRef](#)]
110. Eshgarf, H.; Afrand, M. An experimental study on rheological behavior of non-Newtonian hybrid nano-coolant for application in cooling and heating systems. *Exp. Therm. Fluid Sci.* **2016**, *76*, 221–227. [[CrossRef](#)]
111. Sundar, L.S.; Ramana, E.V.; Graça, M.; Singh, M.K.; Sousa, A.C.J. Nanodiamond- Fe_3O_4 nanofluids: Preparation and measurement of viscosity, electrical and thermal conductivities. *Int. Commun. Heat Mass Transf.* **2016**, *73*, 62–74. [[CrossRef](#)]
112. Soltani, O.; Akbari, M. Effects of temperature and particles concentration on the dynamic viscosity of MgO-MWCNT/ethylene glycol hybrid nanofluid: Experimental study. *Phys. E Low-Dimens. Syst. Nanostruct.* **2016**, *84*, 564–570. [[CrossRef](#)]
113. Senniangiri, N.; Bensam Raj, J.; Sunil, J.J. Effects of temperature and particles concentration on the dynamic viscosity of graphene-NiO/coconut oil hybrid nanofluid: Experimental study. *Int. J. Nanosci.* **2020**, *19*, 1950016. [[CrossRef](#)]
114. Nemade, K.; Waghuley, S.J. A novel approach for enhancement of thermal conductivity of CuO/ H_2O based nanofluids. *Appl. Therm. Eng.* **2016**, *95*, 271–274. [[CrossRef](#)]
115. Verma, S.K.; Tiwari, A.K.; Tiwari, S.; Chauhan, D.S. Performance analysis of hybrid nanofluids in flat plate solar collector as an advanced working fluid. *Sol. Energy* **2018**, *167*, 231–241. [[CrossRef](#)]
116. Arıkan, E.; Abbasoğlu, S.; Gazi, M. Experimental performance analysis of flat plate solar collectors using different nanofluids. *Sustainability* **2018**, *10*, 1794. [[CrossRef](#)]
117. Sabiha, M.; Saidur, R.; Hassani, S.; Said, Z.; Mekhilef, S. Energy performance of an evacuated tube solar collector using single walled carbon nanotubes nanofluids. *Energy Convers. Manag.* **2015**, *105*, 1377–1388. [[CrossRef](#)]
118. Mahendran, M.; Lee, G.; Sharma, K.; Shahrani, A. Performance of evacuated tube solar collector using water-based titanium oxide nanofluid. *J. Mech. Eng. Sci.* **2012**, *3*, 301–310. [[CrossRef](#)]
119. Daghigh, R.; Zandi, P. Improving the performance of heat pipe embedded evacuated tube collector with nanofluids and auxiliary gas system. *Renew. Energy* **2018**, *134*, 888–901. [[CrossRef](#)]
120. Peng, Y.; Zahedidastjerdi, A.; Abdollahi, A.; Amindoust, A.; Bahrami, M.; Karimipour, A.; Goodarzi, M. Investigation of energy performance in a U-shaped evacuated solar tube collector using oxide added nanoparticles through the emitter, absorber and transmittal environments via discrete ordinates radiation method. *J. Therm. Anal.* **2019**, *139*, 2623–2631. [[CrossRef](#)]
121. Luo, Z.; Wang, C.; Wei, W.; Xiao, G.; Ni, M. Performance improvement of a nanofluid solar collector based on direct absorption collection (DAC) concepts. *Int. J. Heat Mass Transf.* **2014**, *75*, 262–271. [[CrossRef](#)]
122. Hussain, H.A.; Jawad, Q.; Sultan, K.F. Experimental analysis on thermal efficiency of evacuated tube solar collector by using nanofluids. *Sol. Energy* **2015**, *4*, 19–28.
123. Kim, H.; Ham, J.; Park, C.; Cho, H. Theoretical investigation of the efficiency of a U-tube solar collector using various nanofluids. *Energy* **2016**, *94*, 497–507. [[CrossRef](#)]
124. Kaya, M.; Gürel, A.E.; Ağbulut, Ü.; Ceylan, İ.; Çelik, S.; Ergün, A.; Acar, B.J. Performance analysis of using CuO-Methanol nanofluid in a hybrid system with concentrated air collector and vacuum tube heat pipe. *Energy Convers. Manag.* **2019**, *199*, 111936. [[CrossRef](#)]
125. Benkhedda, M.; Boufendi, T.; Touahri, S.J. Laminar mixed convective heat transfer enhancement by using Ag- TiO_2 -water hybrid Nanofluid in a heated horizontal annulus. *Heat Mass Transf.* **2018**, *54*, 2799–2814. [[CrossRef](#)]
126. Rahman, M.R.A.; Leong, K.Y.; Idris, A.C.; Saad, M.R.; Anwar, M. Numerical analysis of the forced convective heat transfer on Al_2O_3 -Cu/water hybrid nanofluid. *Heat Mass Transf.* **2016**, *53*, 1835–1842. [[CrossRef](#)]
127. Gorji, T.B.; Ranjbar, A. A numerical and experimental investigation on the performance of a low-flux direct absorption solar collector (DASC) using graphite, magnetite and silver nanofluids. *Sol. Energy* **2016**, *135*, 493–505. [[CrossRef](#)]

128. Li, X.; Chang, H.; Zeng, L.; Huang, X.; Li, Y.; Li, R.; Xi, Z. Numerical analysis of photothermal conversion performance of MXene nanofluid in direct absorption solar collectors. *Energy Convers. Manag.* **2020**, *226*, 113515. [[CrossRef](#)]
129. Gupta, M.; Singh, V.; Said, Z. Heat transfer analysis using zinc Ferrite/water (Hybrid) nanofluids in a circular tube: An experimental investigation and development of new correlations for thermophysical and heat transfer properties. *Sustain. Energy Technol. Assess.* **2020**, *39*, 100720. [[CrossRef](#)]
130. Abdelrazik, A.S.; Tan, K.H.; Aslfattahi, N.; Saidur, R.; Al-Sulaiman, F.A. Optical properties and stability of water-based nanofluids mixed with reduced graphene oxide decorated with silver and energy performance investigation in hybrid photovoltaic/thermal solar systems. *Int. J. Energy Res.* **2020**, *44*, 11487–11508. [[CrossRef](#)]
131. Kasaeian, A.; Daneshazarian, R.; Pourfayaz, F. Comparative study of different nanofluids applied in a trough collector with glass-glass absorber tube. *J. Mol. Liq.* **2017**, *234*, 315–323. [[CrossRef](#)]
132. Loni, R.; Pavlovic, S.; Bellos, E.; Tzivanidis, C.; Asli-Ardeh, E.A. Thermal and exergy performance of a nanofluid-based solar dish collector with spiral cavity receiver. *Appl. Therm. Eng.* **2018**, *135*, 206–217. [[CrossRef](#)]
133. Esfe, M.H.; Alirezaie, A.; Rejvani, M.J. An applicable study on the thermal conductivity of SWCNT-MgO hybrid nanofluid and price-performance analysis for energy management. *Appl. Therm. Eng.* **2017**, *111*, 1202–1210. [[CrossRef](#)]
134. Asadi, M.; Asadi, A.J. Dynamic viscosity of MWCNT/ZnO-engine oil hybrid nanofluid: An experimental investigation and new correlation in different temperatures and solid concentrations. *Int. Commun. Heat Mass Transf.* **2016**, *76*, 41–45. [[CrossRef](#)]
135. Afrand, M. Experimental study on thermal conductivity of ethylene glycol containing hybrid nano-additives and development of a new correlation. *Appl. Therm. Eng.* **2017**, *110*, 1111–1119. [[CrossRef](#)]
136. Sundar, L.S.; Singh, M.K.; Ferro, M.; Sousa, A. Experimental investigation of the thermal transport properties of graphene oxide/Co₃O₄ hybrid nanofluids. *Int. Commun. Heat Mass Transf.* **2017**, *84*, 1–10. [[CrossRef](#)]
137. Nine, J.; Batmunkh, M.; Kim, J.-H.; Chung, H.-S.; Jeong, H.-M. Investigation of Al₂O₃-MWCNTs hybrid dispersion in water and their thermal characterization. *J. Nanosci. Nanotechnol.* **2012**, *12*, 4553–4559. [[CrossRef](#)] [[PubMed](#)]
138. Khan, M.S.; Abid, M.; Ali, H.M.; Amber, K.P.; Bashir, M.A.; Javed, S. Comparative performance assessment of solar dish assisted s-CO₂ Brayton cycle using nanofluids. *Appl. Therm. Eng.* **2018**, *148*, 295–306. [[CrossRef](#)]
139. Zadeh, P.M.; Sokhansfat, T.; Kasaeian, A.; Kowsary, F.; Akbarzadeh, A. Hybrid optimization algorithm for thermal analysis in a solar parabolic trough collector based on nanofluid. *Energy* **2015**, *82*, 857–864. [[CrossRef](#)]
140. Huang, W.; Marefati, M. Energy, exergy, environmental and economic comparison of various solar thermal systems using water and Therminol B base fluids, and CuO and Al₂O₃ nanofluids. *Energy Rep.* **2020**, *6*, 2919–2947. [[CrossRef](#)]
141. Loni, R.; Asli-Ardeh, E.A.; Ghobadian, B.; Kasaeian, A.; Bellos, E. Energy and exergy investigation of alumina/oil and silica/oil nanofluids in hemispherical cavity receiver: Experimental study. *Energy* **2018**, *164*, 275–287. [[CrossRef](#)]
142. Potenza, M.; Milanese, M.; Colangelo, G.; de Risi, A. Experimental investigation of transparent parabolic trough collector based on gas-phase nanofluid. *Appl. Energy* **2017**, *203*, 560–570. [[CrossRef](#)]
143. Aslfattahi, N.; Samyalingam, L.; Abdelrazik, A.; Arifuzzaman, A.; Saidur, R. MXene based new class of silicone oil nanofluids for the performance improvement of concentrated photovoltaic thermal collector. *Sol. Energy Mater. Sol. Cells* **2020**, *211*, 110526. [[CrossRef](#)]
144. Soltani, S.; Kasaeian, A.; Lavajoo, A.; Loni, R.; Najafi, G.; Mahian, O. Exergetic and environmental assessment of a photovoltaic thermal-thermoelectric system using nanofluids: Indoor experimental tests. *Energy Convers. Manag.* **2020**, *218*, 112907. [[CrossRef](#)]
145. Sardarabadi, M.; Passandideh-Fard, M.; Heris, S.Z. Experimental investigation of the effects of silica/water nanofluid on PV/T (photovoltaic thermal units). *Energy* **2014**, *66*, 264–272. [[CrossRef](#)]
146. Arora, S.; Singh, H.P.; Sahota, L.; Arora, M.K.; Arya, R.; Singh, S.; Jain, A.; Singh, A. Performance and cost analysis of photovoltaic thermal (PVT)-compound parabolic concentrator (CPC) collector integrated solar still using CNT-water based nanofluids. *Desalination* **2020**, *495*, 114595. [[CrossRef](#)]
147. Wahab, A.; Khan, M.A.Z.; Hassan, A. Impact of graphene nanofluid and phase change material on hybrid photovoltaic thermal system: Exergy analysis. *J. Clean. Prod.* **2020**, *277*, 123370. [[CrossRef](#)]
148. Soltani, S.; Kasaeian, A.; Sarrafha, H.; Wen, D. An experimental investigation of a hybrid photovoltaic/thermoelectric system with nanofluid application. *Sol. Energy* **2017**, *155*, 1033–1043. [[CrossRef](#)]
149. Sardarabadi, M.; Hosseinzadeh, M.; Kazemian, A.; Passandideh-Fard, M. Experimental investigation of the effects of using metal-oxides/water nanofluids on a photovoltaic thermal system (PVT) from energy and exergy viewpoints. *Energy* **2017**, *138*, 682–695. [[CrossRef](#)]
150. Sardarabadi, M.; Passandideh-Fard, M.J.S.E.M.; Cells, S. Experimental and numerical study of metal-oxides/water nanofluids as coolant in photovoltaic thermal systems (PVT). *Energy* **2016**, *157*, 533–542. [[CrossRef](#)]
151. Sakhaei, S.A.; Valipour, M.S. Performance enhancement analysis of the flat plate collectors: A comprehensive review. *Renew. Sustain. Energy Rev.* **2018**, *102*, 186–204. [[CrossRef](#)]
152. Duffie, J.A.; Beckman, W.A. *Solar Engineering of Thermal Processes*; John Wiley & Sons: Hoboken, NJ, USA, 2013.
153. Salman, A.; Hamdi, R.J. Theoretical technique for studying the effecting factors for loss coefficients theoretical technique for studying the effecting factors for loss coefficients in solar collectors. *Int. J. Trend Res. Dev.* **2018**, *5*, 1–6.
154. Ward, G.T. Performance of a flat-plate solar heat collector. *Proc. Inst. Mech. Eng.* **1955**, *169*, 1091–1112. [[CrossRef](#)]
155. Klein, S. Calculation of flat-plate collector loss coefficients. *Sol. Energy* **1975**, *17*, 79–80. [[CrossRef](#)]

156. Fudholi, A.; Sopian, K. A review of solar air flat plate collector for drying application. *Renew. Sustain. Energy Rev.* **2018**, *102*, 333–345. [[CrossRef](#)]
157. Golneshan, A.; Nemati, H. Exergy analysis of unglazed transpired solar collectors (UTCs). *Sol. Energy* **2014**, *107*, 272–277. [[CrossRef](#)]
158. Badache, M.; Hallé, S.; Rouse, D. A full 34 factorial experimental design for efficiency optimization of an unglazed transpired solar collector prototype. *Sol. Energy* **2012**, *86*, 2802–2810. [[CrossRef](#)]
159. Leon, M.A.; Kumar, S. Mathematical modeling and thermal performance analysis of unglazed transpired solar collectors. *Sol. Energy* **2007**, *81*, 62–75. [[CrossRef](#)]
160. Kutscher, C.F. Heat exchange effectiveness and pressure drop for air flow through perforated plates with and without crosswind. *J. Heat Transf.* **1994**, *116*, 391–399. [[CrossRef](#)]
161. Esfe, M.H.; Behbahani, P.M.; Arani, A.A.A.; Sarlak, M.R. Thermal conductivity enhancement of SiO₂–MWCNT (85: 15%)–EG hybrid nanofluids. *J. Therm. Anal. Calorim.* **2017**, *128*, 249–258. [[CrossRef](#)]
162. Esfahani, N.N.; Toghraie, D.; Afrand, M.J. A new correlation for predicting the thermal conductivity of ZnO–Ag (50–50%)/water hybrid nanofluid: An experimental study. *Powder Technol.* **2018**, *323*, 367–373. [[CrossRef](#)]
163. Toghraie, D.; Chaharsoghi, V.A.; Afrand, M.J. Measurement of thermal conductivity of ZnO–TiO₂/EG hybrid nanofluid. *J. Therm. Anal. Calorim.* **2016**, *125*, 527–535. [[CrossRef](#)]
164. Alirezaie, A.; Saedodin, S.; Esfe, M.H.; Rostamian, S.H. Investigation of rheological behavior of MWCNT (COOH-functionalized)/MgO-engine oil hybrid nanofluids and modelling the results with artificial neural networks. *J. Mol. Liq.* **2017**, *241*, 173–181. [[CrossRef](#)]
165. Moldoveanu, G.M.; Ibanescu, C.; Danu, M.; Minea, A.A. Viscosity estimation of Al₂O₃, SiO₂ nanofluids and their hybrid: An experimental study. *J. Mol. Liq.* **2018**, *253*, 188–196. [[CrossRef](#)]
166. Motahari, K.; Moghaddam, M.A.; Moradian, M. Experimental investigation and development of new correlation for influences of temperature and concentration on dynamic viscosity of MWCNT–SiO₂ (20–80)/20W50 hybrid nano-lubricant. *Chin. J. Chem. Eng.* **2018**, *26*, 152–158. [[CrossRef](#)]
167. Sajid, M.U.; Ali, H.M.J. Thermal conductivity of hybrid nanofluids: A critical review. *Int. J. Heat Mass Transf.* **2018**, *126*, 211–234. [[CrossRef](#)]
168. Choi, C.; Yoo, H.; Oh, J. Preparation and heat transfer properties of nanoparticle-in-transformer oil dispersions as advanced energy-efficient coolants. *Curr. Appl. Phys.* **2007**, *8*, 710–712. [[CrossRef](#)]
169. Otanicar, T.P.; Phelan, P.E.; Prasher, R.S.; Rosengarten, G.; Taylor, R.A. Nanofluid-based direct absorption solar collector. *J. Renew. Sustain. Energy* **2010**, *2*, 33102. [[CrossRef](#)]
170. Khullar, V.; Tyagi, H.; Phelan, P.; Otanicar, T.; Singh, H.; Taylor, R.A. Solar energy harvesting using nanofluids-based concentrating solar collector. *J. Nanotechnol. Eng. Med.* **2012**, *3*, 31003. [[CrossRef](#)]
171. Sundar, L.S.; Kirubeil, A.; Punnaiah, V.; Singh, M.K.; Sousa, A. Effectiveness analysis of solar flat plate collector with Al₂O₃ water nanofluids and with longitudinal strip inserts. *Int. J. Heat Mass Transf.* **2018**, *127*, 422–435. [[CrossRef](#)]
172. Khaleduzzaman, S.; Sohel, M.; Saidur, R.; Selvaraj, J. Stability of Al₂O₃-water nanofluid for electronics cooling system. *Procedia Eng.* **2015**, *105*, 406–411. [[CrossRef](#)]
173. Shao, X.; Chen, Y.; Mo, S.; Cheng, Z.; Yin, T. Dispersion stability of TiO₂-H₂O nanofluids containing mixed nanotubes and nanosheets. *Energy Procedia* **2015**, *75*, 2049–2054. [[CrossRef](#)]
174. Gorjian, S.; Ebadi, H.; Calise, F.; Shukla, A.; Ingraio, C. A review on recent advancements in performance enhancement techniques for low-temperature solar collectors. *Energy Convers. Manag.* **2020**, *222*, 113246. [[CrossRef](#)]
175. Hamzah, M.H.; Sidik, N.A.C.; Ken, T.L.; Mamat, R.; Najafi, G. Factors affecting the performance of hybrid nanofluids: A comprehensive review. *Int. J. Heat Mass Transf.* **2017**, *115*, 630–646. [[CrossRef](#)]
176. Ma, M.; Zhai, Y.; Yao, P.; Li, Y.; Wang, H. Synergistic mechanism of thermal conductivity enhancement and economic analysis of hybrid nanofluids. *Powder Technol.* **2020**, *373*, 702–715. [[CrossRef](#)]
177. Alirezaie, A.; Hajmohammad, M.H.; Ahangar, M.R.H.; Esfe, M.H. Price-performance evaluation of thermal conductivity enhancement of nanofluids with different particle sizes. *Appl. Therm. Eng.* **2018**, *128*, 373–380. [[CrossRef](#)]